ADDIS ABABA UNIVERSITY

SCHOOL OF GRADUATE STUDIES

FACULTY OF TECHNOLOGY

ELECTRICAL AND COMPUTER ENGINEERING

DEPARTMENT

ENHANCED PEAK-TO-AVERAGE POWER RATIO REDUCTION TECHNIQUE IN OFDM COMMUNICATION SYSTEMS

By

Mengistu Abera

A thesis submitted to the School of Graduate Studies of Addis Ababa University in partial fulfillment of the requirements for the degree of

Masters of Science

In

Electrical Engineering

Date: June 2007 G.C.

Addis Ababa, Ethiopia

ADDIS ABABA UNIVERSITY

SCHOOL OF GRADUATE STUDIES

FACULTY OF TECHNOLOGY

ELECTRICAL AND COMPUTER ENGINEERING

DEPARTMENT

ENHANCED PEAK-TO-AVERAGE POWER RATIO REDUCTION TECHNIQUE IN OFDM COMMUNICATION SYSTEMS

By

Mengistu Abera

Advisor

Dr. Ing. Hailu Ayele

ADDIS ABABA UNIVERSITY

SCHOOL OF GRADUATE STUDIES

FACULTY OF TECHNOLOGY

ENHANCED PEAK-TO-AVERAGE POWER RATIO REDUCTION TECHNIQUE IN OFDM COMMUNICATION SYSTEMS

BY

MENGISTU ABERA

APPROVAL BY BOARD OF EXAMINERS

Chairman Department of Graduate Committee	Signature
Advisor	Signature
Examiner	Signature
External Examiner	Signature

ABSTRACT

The Orthogonal Frequency Division Multiplexing (OFDM) is a strong candidate for the current and future wireless communications system due to its high data rates transmission capability and robustness against multi-path fading effects.
A major drawback of OFDM is its high peak to average power ratio (PAPR). Since most practical transmission systems are peak power limited, the average transmit power should be reduced for linear operation over the full dynamic range, which degrades the received signal power.

In this thesis we review the most popular OFDM PAPR-reduction techniques and demonstrate in detail that Selected Mapping (SLM) scheme is a particularly promising reduction technique. In a SLM system, an OFDM symbol is mapped to a set of independent but equivalent symbols and then the lowest-PAPR symbol is selected for transmission. The tradeoff for PAPR reduction in SLM is computational complexity as each mapping requires an additional inverse fast Fourier transform (IFFT) operation in the transmitter.

An enhanced SLM method is proposed for computational complexity reduction. The proposed SLM scheme transforms an input symbol sequence into a set of OFDM signals by multiplying the phase sequences by the signal after a certain intermediate stage of inverse fast Fourier transform (IFFT).

The enhanced SLM technique reduces computational complexity by 48% while it shows almost the same performance of PAPR reduction as that of the conventional SLM OFDM scheme.

ACKNOWLEDGEMENTS

I want to first thank my advisor, Dr.-Ing. Hailu Ayele, for giving me the chance to do this work, for the encouragement, and for the guidance.

I also appreciate Ms. Tigist Tsegaye, whose patience in typing the whole thesis manuscript adds me great strength. Special thanks to my friends, Amare , Azene , Astatkie , Hailu , Gedion and Daniel, to name only a few.

Last but not least I am greatly indebted to my family, especially to my mother and my brother who always encourage me to attain my goal.

TABLE OF CONTENTS

ABSTRACT…… **i**

ACKNOWLEDGEMENT…… **ii**

TABLE OF CONTENTS……..**iii**

ABRREVIATIONS …… **vi**

CHAPTER I.

INTRODUCTION…….……**1**

1.1. Outline of the thesis……..2

CHAPTER II. OFDM AND THE PAPR PROBLEM……**4**

2.1. Orthogonal Frequency Division Multiplexing (OFDM)……..4

2.2. Serial to Parallel converter……...……5

2.3. The Cyclic Prefix…..……..……...….8

2.4. Discrete-Time Signal Processing of OFDM……...…..9

2.5. Band pass signaling ……..……...9

2.6. OFDM Demodulation ……..…….…10

2.7. Modern OFDM Block Diagram …….…....10

2.8. Problems with OFDM ……..…..11

2.9. Statistics of PAPR …….……14

2.10. PAPR Distribution and Clipping Probability for OFDM Symbols ……..…..15

2.11. Effect of PAPR on Amplifier Efficiency……..……..…..17

CHAPTER III. PAPR REDUCTION TECHNIQUES……..…….……..…**20**

3.1. PAPR Reduction …….……...……20

3.2. Amplitude Clipping……..…….....20

3.3.

Companding……..…….23

3.4. Tone Reservation……..……..25

3.5. Tone Injection……..……...……29

3.6. Partial Transmit Sequence…….…….30
3.7. Selected Mapping …….……...….32
3.8. Comparison of main PAPR reduction techniques.……...…….…..…..33
CHAPTER IV. ENHANCED SELECTED MAPPING TECHNIQUE…….……35
4.1. Conventional Selected Mapping ……...35
4.2. Recovery of data at receiver ……..36
4.3. PAPR calculation using Selected Mapping ……..……...36
4.4. Generation of OFDM frames representing the same information ……38
4.5. Enhanced Selected Mapping ……..…….…….40
4.6. Phase Sequences of enhanced SLM Scheme ……...42
4.7. Hadamard Matrix ……...…….….42
4.8. Computational Complexity ……..42
CHAPTER V. SIMULATION, RESULTS, AND DISCUSSIONS……....**45**
5.1. Conventional Selected Mapping Simulation Model …....……..46
5.2. Complementary Cumulative Distribution Function (CCDF)……47
5.3. Enhanced Selected Mapping Model……..…...49
CHAPTER VI. CONCLUSION AND FUTUR WORK ….……...…..…..*53*
6.1. Conclusion ……...…….....….…….53
6.2. Future work…….…....……54
APPENDIX A: More on the OFDM Literature….……..…55
APPENDIX B: Practical OFDM Example..…….……..…….…… 57
1. DVB-T Example.…….…….……57
2. IFFT Implementation……..……..……...…58
SYMBOLS AND OPERATORS……..…….…60
REFERENCES……..…….……....62

Declaration

I, the undersigned, declare that this thesis is my original work, has not been presented for a degree in this or any other university, and all sources of materials used for the thesis have been acknowledged.

Name: Mengistu Abera

Signature: _____

Place: Addis Ababa

Date of submission: _____

This thesis has been submitted for examination with my approval as a university advisor.

Dr.-Ing. Hailu Ayele _____

Advisor's Name Signature

CHAPTER I

INTRODUCTION

Humans have always found ways to communicate, over space and over time.

From the message in a bottle to cave drawings, smoke signals and beacons, people have used inventive techniques, techniques derived from their natural environment, to share information among people at different locations. A good natural resource for communication is electricity for its speed and ability to be controlled with devices like capacitors, microprocessors, electronic memory storage. Communication was greatly enhanced with Morse's telegraph (1837), Bell's telephone (1876), Edison's phonograph (1887), and Marconi's radio (1896). From these early inventions, communications technology has advanced with global telephone networks, satellite communications, and magnetic storage systems; and with the rise of the internet and digital computers, digital communications—the transfer of bits (1's and 0's) from one point to another—has become important.

In particular, wireless digital communications is currently under intensive research, and development to provide high data rate access. The demand for high data rate services has been increasing very rapidly. Almost every existing physical medium capable of supporting broadband data transmission to our homes, offices and schools has been or will be used in the future. This includes both wired (Digital subscriber lines, power lines) and wireless media. These services require very reliable transmission over very harsh environments. The transmission systems experience many degradations, such as noise, multipath, interference, nonlinearities, and should meet certain constraints such as limited transmit power and cost. One technique that has currently gained much popularity due to its robustness in dealing with the major current wireless problems is Orthogonal frequency division multiplexing (OFDM).

Unfortunately, one major problem with orthogonal frequency division multiplexing signals is its large envelope variations which is quantified by the parameter called Peak to average power ratio (PAPR). Like any other systems, communication systems are peak power limited as they involve nonlinear devices. So a system should be designed to operate at power levels below the maximum power available.

The high PAPR in the OFDM signal, often in excess of 10 dB, driving the power amplifier to operate in the nonlinear region, which causes distortion of the OFDM signal [33]. The high PAPR will also increase the complexity of the A/D and D/A converters and it reduces the transmitter's power efficiency.

One way to avoid nonlinear distortion is to use power amplifier (PA) with large linear range, which is a challenge for the power amplifier designer. Another way is to change the OFDM signals by processing the signal before the power amplifier to make sure that the input signal lies in the linear region of the PA. Usually, to avoid operating the amplifiers with large back-offs occasional saturation of the power amplifiers or clipping in the digital to analogue converters must be allowed. This creates additional nonlinearity distortion that increases the bit error rate in receivers, and also causes spectral widening of the transmit signal that increases adjacent channel interference to other users. In this thesis, the major PAPR reduction techniques are surveyed.

1.1 Outline of the thesis

Chapter 2 introduces OFDM and the PAPR problem. The fundamental theories behind this thesis are described. The complementary cumulative distribution function (CCDF) will be discussed in the same chapter.

Chapter 3 describes PAPR reduction techniques and gives some more detail on the major PAPR reduction methods: Amplitude Clipping, Companding, Tone Reservation (TR), Tone Injection (TI), Partial Transmit Sequence (PTS) and Selected Mapping (SLM). Finally, Comparison of these PAPR reduction techniques based on side information needed, data rate reduction, BER increase and computational complexity is made so as to select the most effective PAPR reduction technique for further enhancement.

Chapter 4 presents the Selected Mapping (conventional SLM) PAPR reduction technique. The new or enhanced selected mapping technique which is mainly focused on reducing the computational complexity of conventional selected mapping technique is detailed in the same chapter. The theoretical simulation plots and the computational complexity calculations for the conventional and enhanced SLM techniques are also shown in this chapter.

Chapter 5 addresses the simulation results of both conventional and enhanced selected mapping techniques. The simulation is made for the OFDM digital video

broadcasting terrestrial (DVB-T) system of the IEEE standard 802.16 [27] intended for mobile reception of digital TV.

Finally, in Chapter 6, conclusions are presented and possible improvements of the systems and future work are proposed.

CHAPTER II

OFDM AND THE PAPR PROBLEM

In this chapter, modern OFDM system block diagram will be discussed. The principal model as well as the mathematical formulae will be addressed to overview the advantages of the OFDM modulation technique over other schemes. Together with this, the major OFDM problem (the high peak-to-average power ratio) will be detailed.

2.1 Orthogonal Frequency Division Multiplexing (OFDM)

The original OFDM was proposed in the 1960s [13]. The key idea of OFDM is that a single user would make use of all orthogonal subcarriers in divided frequency bands. So that the data rate can be increased significantly. Since the bandwidth is divided into several narrower subchannels, each subchannel requires a longer symbol period. As a result OFDM system can overcome the intersymbol interference (ISI) problem. Therefore, the OFDM symbol can result in lower bit error rates (BER) and high data rates than the conventional communication systems.

Therefore, to meet the current and future demanding data rate requirements, OFDM modulation technique has become exceedingly popular. OFDM has been implemented in diverse applications such as digital subscriber lines (xDSL) [14], in wireless broadcast applications such as digital audio and video broadcasting (DAB and DVB). It has been used in wireless local area networks (LANs) under the IEEE 802.11. OFDM is being developed for ultra-wideband (UWB) systems; cellular systems; wireless metropolitan area networks (MANs), under the IEEE 802.16 standard; and for other wireline systems such as power line communication (PLC) [15].

OFDM scheme is based on the concept of channel partitioning. i.e, the available transmission bandwidth BW is split into a set of parallel and ideally independent narrowband sub-channels. That means instead of sending data in serial on one channel, data are sent in parallel over N channels, each one being modulated by a low data rate stream. The symbol duration for a OFDM scheme is T. All sub-channels are narrow-band and because of this the channels look like almost flat fading, which makes equalization very simple [1]. Figure 2.1 shows a model of OFDM.

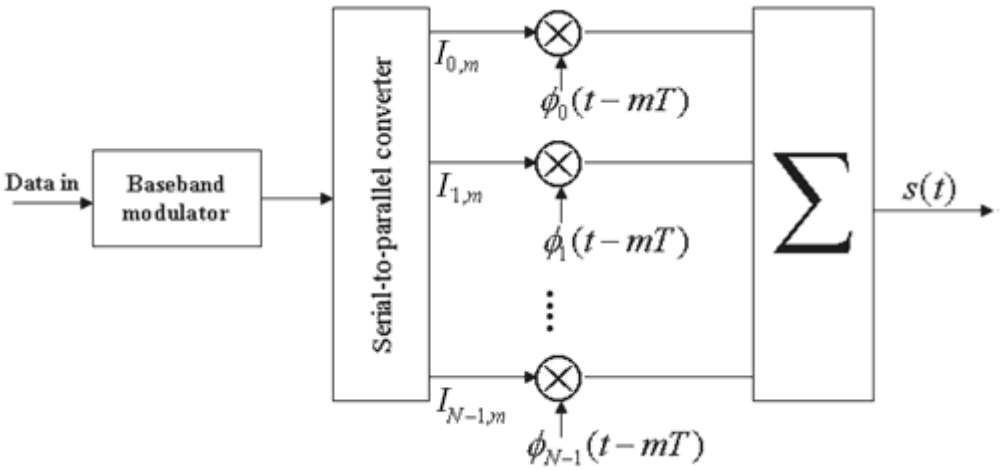

Figure 2.1: OFDM model with N sub-carriers.

The above figure shows that the data stream are modulated into symbols with symbol duration Ts and the symbols will be divided and placed on each sub-carrier by a Series to Parallel (S/P) converter.

2.2 Serial to Parallel (S/P) converter.

The serial to parallel conversion is depicted in figure 2.2

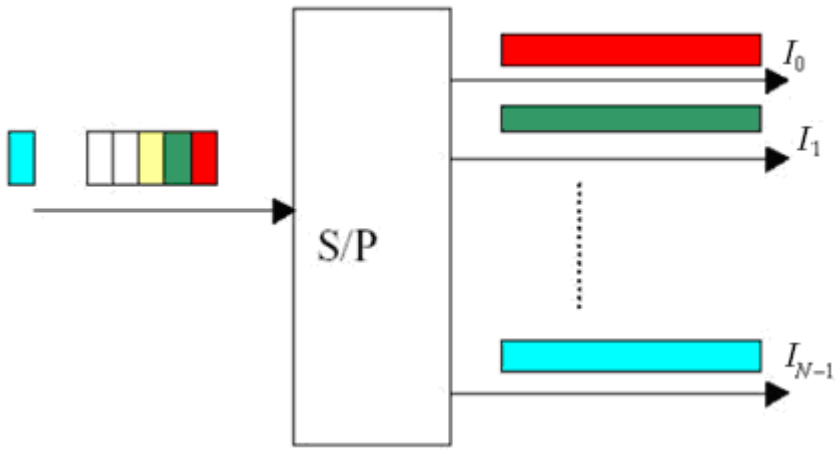

Fig. 2.2 Serial to parallel conversion

Each sub-carrier uses a specific pulse Φ(t − kT), where T = NTs, to modulate the symbols and all the modulated symbols are summed. In the general form, an OFDM signal can be written as the sum of modulated carriers [2], that is

$$s(t) = \sum_{m=-\infty}^{+\infty} \left(\sum_{k=0}^{N-1} I_{k,m} \Phi_k \left(t - mT \right) \right), \ \Phi_k (t - mT) = \left\{ \exp(j2\pi f_c (t - mT)) \right\}_{k=0}^{N-1} \quad (1)$$

Where $I_{k,m}$ is the data symbol modulating the k^{th} sub-carrier in the m^{th} signaling interval. The set of complex sinusoids $\Phi_k (t - mT)$ are referred to as subcarriers. The center frequency of the k^{th} subcarrier is $f_k = k/T_B$ and the subcarrier spacing, $1/T_B$ Hz, makes the subcarriers orthogonal over the block interval, expressed mathematically as

$$\frac{1}{T_B} \int_0^{T_B} \left(e^{j2\pi f_{k1} t} \right)^* \left(e^{j2\pi f_{k2} t} \right) dt = \frac{1}{T_B} \int_0^{T_B} e^{j2\pi \left(f_{k2} - f_{k1} \right) t} dt \quad (2)$$

$$= \begin{cases} 1 & , \ k_1 = k_2 \\ 0 & , k_1 \neq k_2 \end{cases} \quad (3)$$

Where $T_B = NT$ $(\cdot)^*$ represents the complex conjugate operation. The subcarrier orthogonality can also be viewed in the frequency domain.

Consider the 0^{th} OFDM block:

$$s(t) = \sum_{k=0}^{N-1} I_{k,0} e^{j2\pi f_k t} \ , \quad 0 \leq t < T_B \quad (4)$$

The frequency-domain representation is

$$S(f) = F\{s(t)\}(f) = T_B e^{-j2\pi f T_B/2} \sum_{k=0}^{N-1} I_{k,0} \operatorname{sinc} \left[\left(f - \frac{k}{T_B} \right) T_B \right] \quad (5)$$

Where $F\{.\}(f)$ is the Fourier transform and

$$sinc(x) = \begin{cases} 1 & , \ x = 0 \\ \frac{\sin \pi x}{\pi x} & , otherwise \end{cases} \quad (6)$$

Figure 2.3 plots $|S(f)/T_B|$ for N = 16 subcarriers and data symbols with normalized amplitudes. The individual subcarrier spectra are also plotted. Notice that at the k^{th}

subcarrier frequency, k/T_B, the k^{th} subcarrier has a peak and all the other subcarriers have zero-crossings. Therefore, the subcarriers, while tightly packed (which improves spectral efficiency), are non-interfering (i.e. orthogonal). Figure 2.3 also demonstrates that OFDM is a multicarrier modulation. In general, a transmitted bandpass signal is [16].

$$x(t) = \Re\{s(t)e^{j2\pi f_c t}\}, \tag{7}$$

Where f_c is the carrier frequency. For single carrier,

$$x_{sc}(t) = \sum_m |I_m| \cos[2\pi f_c t + \arg(I_m)] g(t - mT) \tag{8}$$

g(t) is the transmit pulse shape. For multicarrier,

$$x_{mc}(t) = \sum_m \{\sum_{k=0}^{N-1} |I_{k,m}| \cos[2\pi (f_c - \frac{k}{T_B})t + \arg(I_{k,m})]\} g(t - mT_B) \tag{9}$$

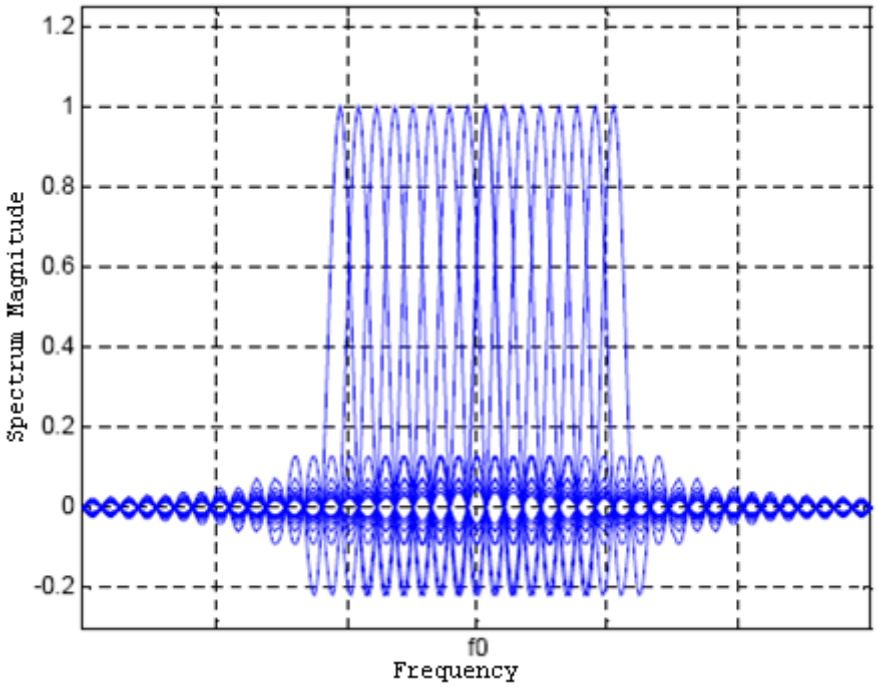

Figure 2.3: Basis of an OFDM signal with N=16 carriers represented in frequency domain.

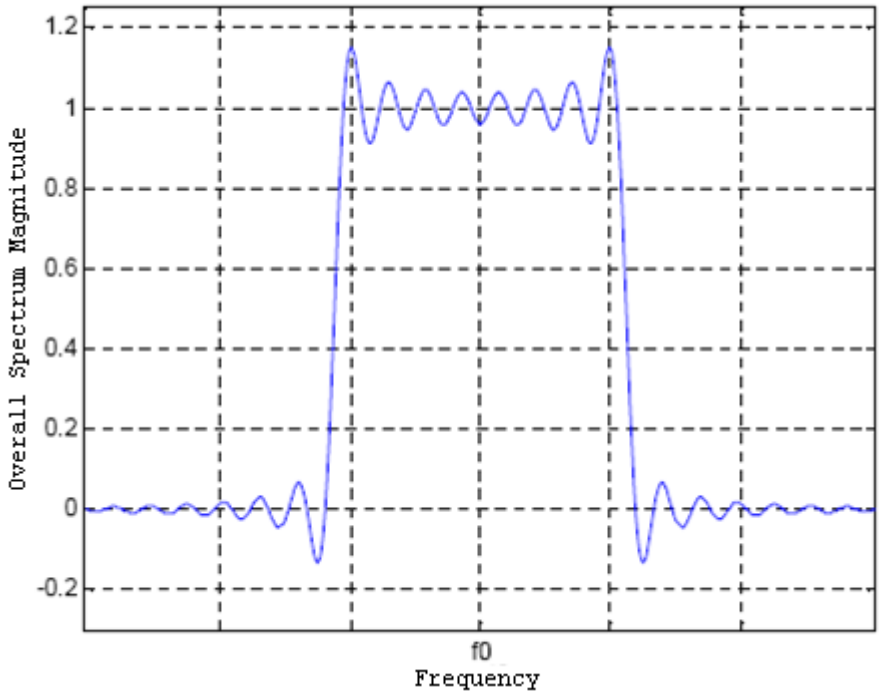

Figure 2.4 - Resulting spectrum from the basis functions of figure 2.3

For single carrier each symbol occupies the entire signal bandwidth, while for multicarrier the bandwidth is split into many frequency bands (also referred to as frequency bins). Notice that the multicarrier signal transmits the N data symbols in parallel over multiple carriers each centered at $(f_c + k/T_B)$ Hz, k = 0, 1, . . . ,N− 1. By properly designing the subcarrier spacing, each frequency bin is made frequency nonselective. The wideband frequency-selective channel is converted into N contiguous narrow band frequency-nonselective bins.

2.3 The Cyclic Prefix

OFDM's main advantage is that it supports high data rate links without requiring a bank of equalizers. Instead of transmitting symbols serially, OFDM sends N symbols as a block. When an OFDM signal passes through a fading channel with response h(t), the orthogonality of the subcarriers will be destroyed which results in Intercarrier interference (ICI). Another problem is multipath propagation which results in ISI. To avoid ISI , cyclic prefix is used in OFDM system. A cyclic prefix is a copy of the last elements of the OFDM symbol added to the beginning of the OFDM symbol and will be removed at the receiver before the demodulation. Figure 2.5 shows the idea with Cyclic Prefix. The OFDM block period, T_B, is thus N times longer than the symbol

period. The interval duration, T_g, is designed such that $T_g \geq \tau_{max}$ so that the channel is absorbed in the guard interval and the OFDM block is uncorrupted. τ_{max} is delay spread. This is illustrated in the figure below.

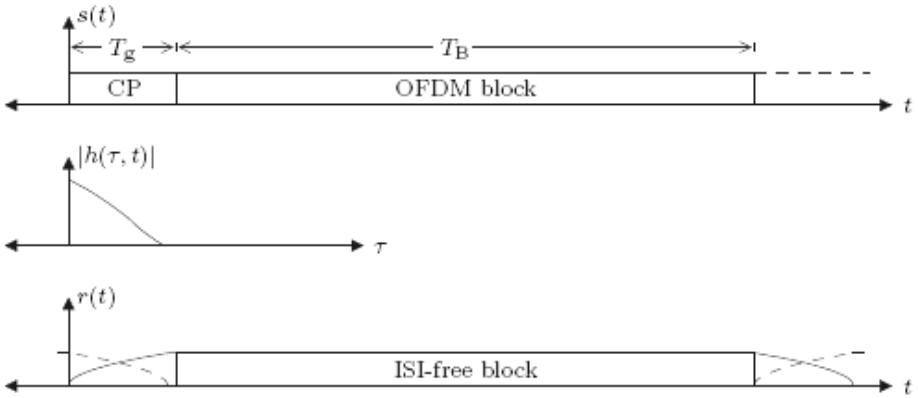

Figure 2.5: OFDM with cyclic prefix (CP).

2.4 Discrete-Time Signal Processing of OFDM

Thus far, two of OFDM's primary advantages have been discussed: the elimination of ISI and the ability to handle large data rate. The other advantage of OFDM is that the modulation and demodulation is done in the discrete-time domain with the inverse fast Fourier transform (IFFT) and fast Fourier transforms (FFT), respectively.

This is seen by sampling s(t) at N equally spaced time instances:

$$y[i] = s(t)\Big|_{t=\frac{iT}{N}} = \sum_{k=0}^{N-1} I_{k,0} e^{j2\pi ki/N}, \qquad i = 0,1,...N-1 \tag{10}$$

which is the inverse discrete Fourier transform (IDFT) of the symbol vector $I_0 = [I_{0,0}, I_{0,1}, \ldots, I_{0,N-1}]$. Different modulation schemes like Binary Phase Shift Keying (BPSK), Quadrature Phase Shift Keying (QPSK), M-array Quadrature Amplitude Modulation (MQAM) and etc are used to modulate the data stream.

Therefore, s (t) is generated at the transmitter with an IDFT followed by a digital-to-analog (D/A) converter.

2.5 Band pass signaling

After modulation by orthogonal subcarriers, all N subcarrier wave forms are added together to be up converted to the pass band. The resulting signal wave form will be transmitted with a carrier frequency at 2.4 GHz, 5 GHz, 11GHz or more based on

applications. Then the band pass OFDM signal wave form would be sent to power amplifier and antennas. Thus, the transmitted OFDM signal x(t) can be expressed as:

$$x(t) = \sum_{n=0}^{N-1} \frac{\exp(j2\pi(f_c + n\Delta f)t)}{\sqrt{T}} s(n), \quad (11)$$

Where Δf is the frequency spacing and the s(n) represents the input data stream, T the symbol duration and f_c the carrier frequency.

2.6 OFDM Demodulation

At the receiver, the received signal is down converted to form a base band signal first. Then, low-pass filter and demodulation are applied to separate subcarrier waveforms. Orthogonality of subcarriers will ensure that only the targeted subcarrier waveform will be preserved in each sub-band.

2.7 Modern OFDM Block Diagram

In general, the input data symbols are complex numbers which result from mapping the bits to points on the complex plane. Next, the symbols are serial to parallel (s/p) converted and processed by the IDFT. The cyclic prefix is added and the signal samples x[i] are passed through the digital to analog (D/A) converter to obtain the continuous time OFDM signal s (t). Finally, the signal is amplified and transmitted. At the receiver, the inverse operations (shown in the figure) are performed.

The modern OFDM block diagram is shown in fig. 2.6

The frequency-domain symbols $\{I_{k,0}\}_{k=0}^{N-1}$ can be expressed as

$$I_{k,0} = \frac{1}{N} \sum_{i=0}^{N-1} y[i] e^{-j2\pi ki/N} \quad , \quad k = 0,1,\cdots,N-1 \quad (12)$$

which is the discrete Fourier transform (DFT) performed on the time-domain samples. The IDFT/DFT is performed efficiently with IFFT/FFT algorithms. Doing so is much simpler than performing the modulation/demodulation in the continuous-time domain with N orthogonally tuned oscillators. Moreover, the signal processing can be performed in software, making OFDM suitable for software defined radios [1].

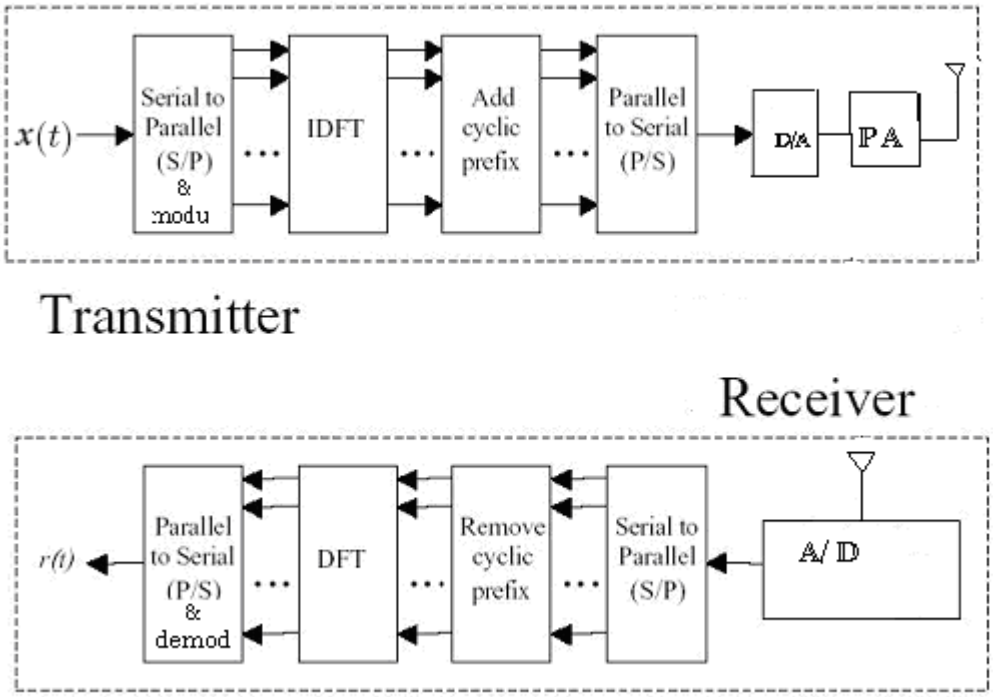

Fig 2.6 Modern OFDM system

2.8 Problems with OFDM

OFDM has two primary drawbacks. The first is sensitivity to imperfect frequency synchronization which is common for mobile applications. This sensitivity arises from the close subcarrier spacing. Figure 2.3 shows that the subcarriers are properly orthogonal at $f = k/T_B$, $k = 0, 1, \ldots, N-1$. However, if the frequency synthesizer at the receiver is misaligned by, say, ϵ_{fo}/T_B Hz, where $-0.5 < \epsilon_{fo} < 0.5$, the subcarriers are not orthogonal and therefore interfering with one another occurs. This intercarrier interference (ICI) is illustrated in Figure 2.8: assuming that the receiver is tuned to $(k + \epsilon_{fo})/T_B$ Hz rather than at the ideal k/T_B Hz, the $N-1$ neighboring subcarriers interfere with the demodulation of the k^{th} subcarrier. The intercarrier interference causes ISI—and potentially high irreducible error floors.

The second problem with OFDM is that the signal has large amplitude fluctuations caused by the summation of the complex sinusoids. Since a large number of waveforms are multiplexed, the peak power continuously increases as the number of carriers, N increases. This effect is seen in figure 2.7.

PAPR ~ the number of carriers N

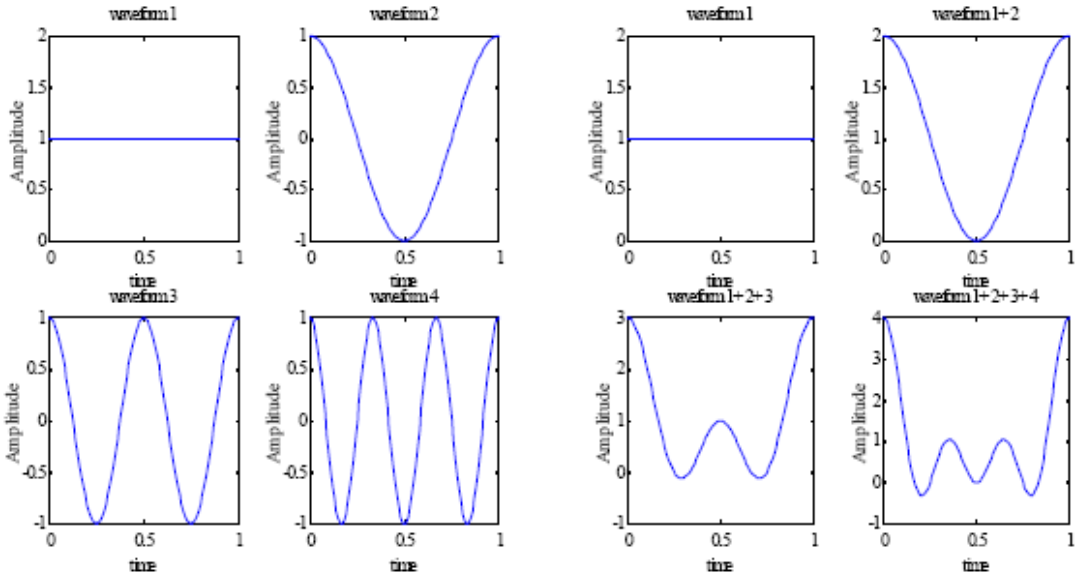

Figure 2.7: Peak variation with number of carriers N

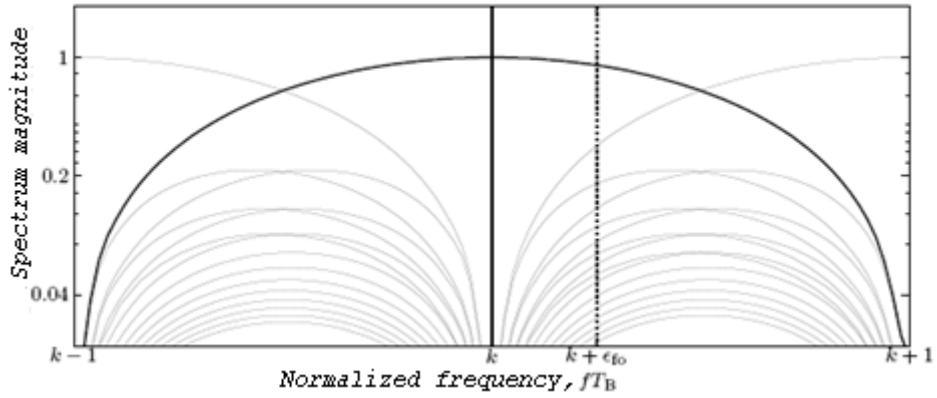

Figure 2.8: Frequency offset causes ICI. (ϵ_{fo}=0.25)

The real and imaginary part of the OFDM signal is

$$\Re\{s(t)\} = \sum_{k=0}^{N-1} \Re\{\boldsymbol{I}_{k,0}\} \cos(\frac{2\pi kt}{T_B}) - \Im\{\boldsymbol{I}_{k,0}\} \sin(\frac{2\pi kt}{T_B}), \tag{13}$$

And

$$\Im\{s(t)\} = \sum_{k=0}^{N-1} \Re\{\boldsymbol{I}_{k,0}\} \sin(\frac{2\pi kt}{T_B}) + \Im\{\boldsymbol{I}_{k,0}\} \cos(\frac{2\pi kt}{T_B}) \tag{14}$$

respectively. Figure 2.9(a) shows the real and imaginary parts of an example OFDM signal with N = 16 subcarriers. Also plotted are the individually modulated sinusoids.

Notice that each sinusoids has a constant amplitude, but when summing the sinusoids the resulting OFDM signal fluctuates over a large range. The instantaneous signal power, $|s(t)|^2 = R^2\{s(t)\} + =I^2\{s(t)\}$, is plotted in Figure 2.9(b). The ratio between the peak power and the average power is 144/16 = 9 (or in decibels, 10 log10 9 ≈ 9.5 dB).

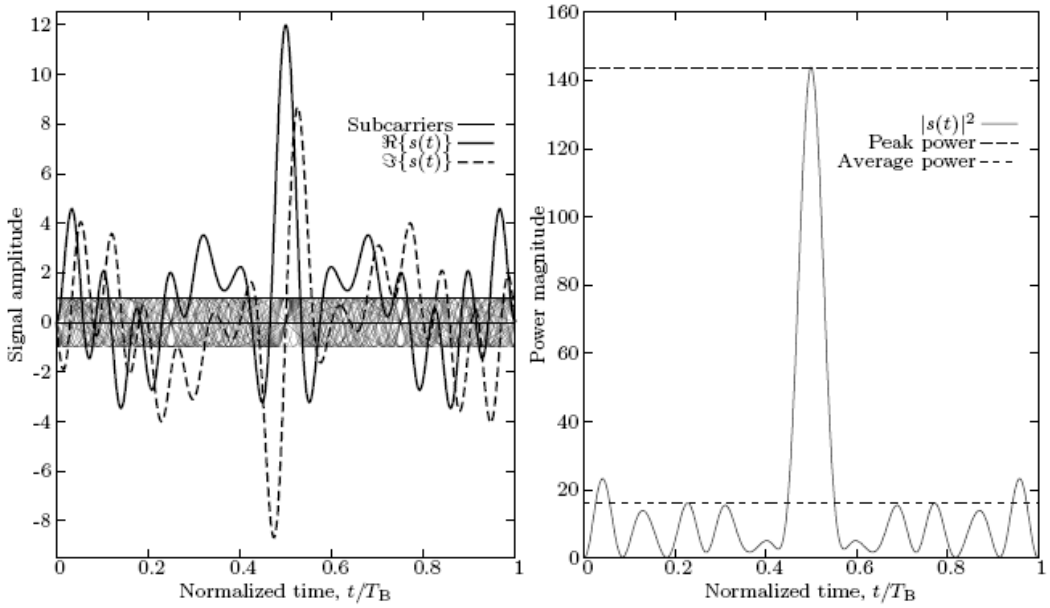

(a) Signal amplitude. **(b) Signal power.**

Figure 2.9: A typical OFDM signal (N = 16). The PAPR is 9.5 dB.

OFDM's high peak-to-average power ratio (PAPR) requires system components with a large linear range capable of accommodating the signal. Otherwise, the circuitry distorts the waveform nonlinearly, and nonlinear distortion results in a loss of subcarrier orthogonality which degrades performance. One such nonlinear device is the transmitter's power amplifier (PA) which is responsible for the system's operational range [35]. Ideally the output of the PA is equal to the input times a gain factor. In reality the PA has a limited linear region, beyond which it saturates to a maximum output level.

Figure 2.10 shows a representative input/output curve. In the linear region the curve matches the ideal, but as the input power increases the PA saturates. The most efficient operating point is at the PA's saturation point, but for signals with large PAPR the operating point must shift to the left keeping the amplification linear. The average input power is reduced and consequently this technique is called input power backoff

(IBO). To keep the peak power of the input signal less than or equal to the saturation input level, the IBO must be at least equal to the PAPR. Thus the required IBO for the OFDM signal in Figure 2.9 is 9.5 dB. At this backoff, the efficiency of a power amplifier decreases significantly. Such an efficiency is detrimental to mobile battery-powered devices which have limited power resources.

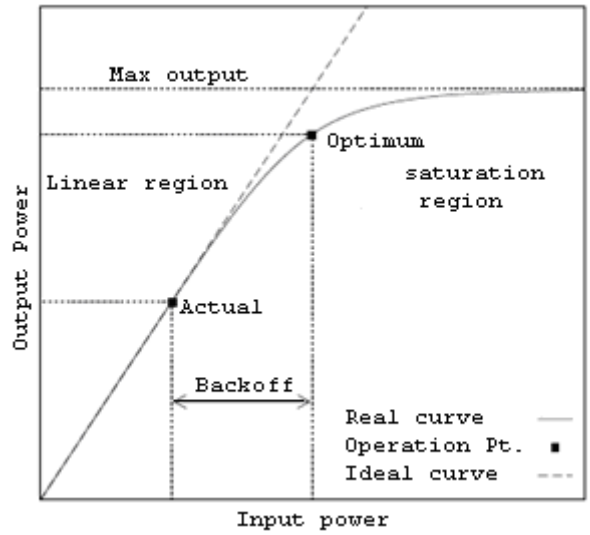

Figure 2.10: Power amplifier transfer function.

Nonlinearities in the transmitter also cause the generation of new frequencies in the transmitted signal. This intermodulation distortion causes interference among the subcarriers, and a broadening of the overall signal spectrum. The spectrum regrowth by in turn causes interference between neighboring systems, an effect known as *adjacent channel interference*.

2.9 Statistics of PAPR

PAPR is the most popular quantification metric for envelope variation of the OFDM signals. It is defined as the ratio of the maximum instantaneous power to the average power of an OFDM signal.

$$PAPR = \frac{Max\left\{\left|\chi_i\right|^2\right\}}{E\left\{\left|\chi_i\right|^2\right\}} \tag{15}$$

where $E[.]$ denotes the expected value and X be any signal representation (critically sampled baseband, oversampled base-band, continuous-time pass band, etc.) defined over one symbol period.

2.10 PAPR Distribution and Clipping Probability for OFDM Symbols

To determine the distribution of PAPR values for an OFDM symbol, we begin with the discrete-time frequency samples which correspond to the values in each frequency bin. The amplitudes and phases of the frequency bins of an OFDM constellation are chosen from an M-QAM constellation. Each time sample of the OFDM symbol is

$$x[n] = \sum_{k=0}^{N-1} X\left(f_k\right) e^{j2\pi kn/N}, \tag{16}$$

where x[n] is the value of the n^{th} time sample, and $X(f_k)$ is the value of the k^{th} frequency bin of the OFDM symbol. The values of $X(\cdot)$ are the amplitude and phase values from the input constellation for that bin. We can model these values as independent random variables, each of which has a finite variance due to the finite constellation size. The values of x[n] will then approach a zero mean, circularly-symmetric complex Gaussian distribution by the Central Limit Theorem.

The magnitude r of a zero-mean complex Gaussian random variable x is therefore a Rayleigh distributed with

$$p_r(r) = \frac{r}{\sigma^2} e^{-\frac{r^2}{2\sigma^2}}, \tag{17}$$

where $2\sigma^2$ is the variance of x. To determine the clipping probability, we note that an OFDM symbol will not be clipped if all of its time samples are less than the clipping threshold say *v*. The probability that the magnitude of a single sample is greater than the clipping threshold *v* is

$$\Pr(r > v) = \int_v^\infty \Pr(r)dr \quad = \quad e^{-\frac{v^2}{2\sigma^2}} \tag{18}$$

The probability of a clip, or that at least one of the time samples of an OFDM symbol of length N is greater than the clipping threshold is therefore,

$$\Pr(\text{clip}) = \Pr(\text{PAPR} > \text{PAPR}_0)$$

$$= 1 - \prod_{i=1}^{N} \Pr\left(\left\|x[i]\right\|^2 < v\right)$$

$$= 1 - \left(1 - \Pr\left(r > v\right)\right)^N$$

$$= 1 - \left(1 - e^{-\frac{v^2}{2\sigma^2}}\right)^N . \qquad (19)$$

The largest amplitude is v, making the peak power v^2, and the average power is the variance of x[n]. Thus the peak-to-average power is the exponent of the exponential of (19), therefore

$$\Pr(\text{PAPR} > \text{PAPR}_0) = 1 - \left(1 - e^{-PAPR_O}\right)^N \qquad (20)$$

is the Complimentary Cumulative Distribution Function (CCDF) of the PAPR of a discrete-time OFDM symbol. Figure 2.11 is a plot of the PAPR of $x[n]$ for different N. It is obvious that at all probability levels the PAPR increases with N.

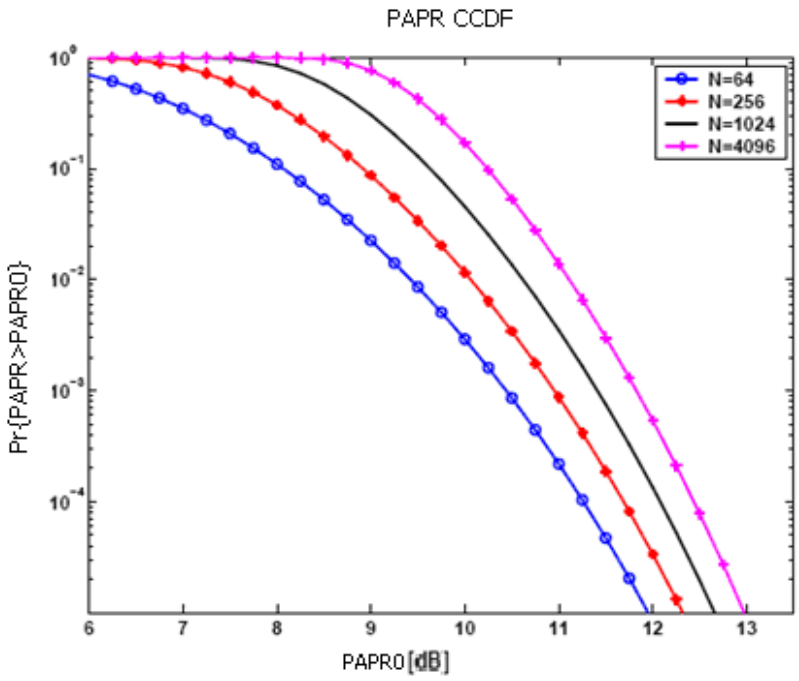

Figure 2.11: CCDF of the discrete-time PAPR for various values of *N*.

PAPR is of the most important in an OFDM system design. For instance, when an engineer has to specify the dynamic range of the digital-to-analog converter (D/A) in an OFDM system, the most important PAPR measurement would be that of the signal input to the D/A which is $x[n]$. On the other hand, the power amplifier will have to be

designed around the PAPR of the passband signal $x_{pb}(t) = R\{x(t)\, e^{j2\pi fct}\}$, where f_c is the carrier frequency. If $fc >> B$, which is the case in most practical systems, then

$$\max|\, x_{pb}(t)| \approx \max\, |x(t)| \,. \tag{21}$$

Also,
$$E\left[\left|x_{pb}(t)\right|^2\right] = E\left[\left|\Re\{x(t)e^{j2\pi f_c t}\right|^2\right]$$

$$= E\left[\Re\left\{x(t)\right\}^2 \cos^2(2\pi f_c t) + \Im\left\{x(t)\right\}^2 \sin^2(2\pi f_c t)\right]$$

$$= \frac{1}{2} E\left[\Re\left\{x(t)\right\}^2 + \Im\left\{x(t)\right\}^2\right]$$

$$= \frac{1}{2} E\left[\left|x(t)\right|^2\right] \;; \tag{22}$$

Therefore,

$$PAPR\left\{x_{pb}(t)\right\} \approx 2PAPR\left\{x(t)\right\} \quad . \tag{23}$$

Equation 20 is a very good approximation to the PAPR distribution of $x[n]$, but differs by as much as one dB from the PAPR distribution of $x(t)$. Several attempts have been made to determine the distribution of $x(t)$. The first attempt is found in [18], where it was shown that

$$\Pr[PAPR\{x(t)\} > PAPR_0] \approx 1 - (1 - e^{-PAPR_0})^{2.8N} \;, \tag{24}$$

which is just a modification to the CCDF that resulted from the Gaussian approximation in (20). Again in [17], some theoretical analysis of the problem was done based on level crossing probabilities of $x_{pb}(t)$, where the ratio fc/B was taken into account as well as the power distribution of $X[k]$. They concluded that for $fc >> B$ and a constant modulus power distribution that (say $PAPR_0 = \gamma$)

$$\Pr[PAPR\{x(t)\} > PAPR_0] \leq N\sqrt{\frac{\pi}{3}\gamma}e^{-\gamma}. \tag{25}$$

2.11 Effect of PAPR on Amplifier Efficiency

Since the amplitude and phase of each frequency bin of an OFDM symbol are independently chosen, the corresponding time waveform can be very peaky especially if the same constellation point is chosen in all the frequency bins. The time waveform will have a single peak at the first sample, and all other samples will be zero. Assuming N subcarriers, that gives a peak power proportional to N^2, and an average

power proportional to N, resulting in a PAPR that is proportional to N. For a typical number of subcarriers, such a large peak to average power ratio can greatly reduce the average efficiency of the transmitter power amplifiers.

For example, Figure 2.12 shows three sample OFDM symbols each comprised of 128 frequency bins using points from a 16-QAM constellation. The amplitudes are plotted relative to the RMS amplitude, so that the average power level corresponds to a relative amplitude of one. The middle plot shows a "typical" OFDM symbol, with a PAPR near the average value of about 7.4 dB. The entire signal is very peaky, with several amplitude peaks that stand out. The highest peak has a relative amplitude of about 2.34, which corresponds to a peak power that is about 5.5 times the average power, resulting in a PAPR of about 7.4 dB. The left plot represents a "good" case, in which the PAPR is almost 3 dB less than the average value. Here one can see that the peaks are almost uniform in height. The right plot shows a "bad" OFDM symbol, with a single very large peak. Clearly in this case, the particular values of the data stream have caused a very unfavorable OFDM symbol in terms of PAPR. Therefore, for these symbols significant SNR margin may be needed to prevent amplifier saturation. The high value of the peak power requires the input of the power amplifier to be scaled so that the peak power does not cause the amplifier to saturate.

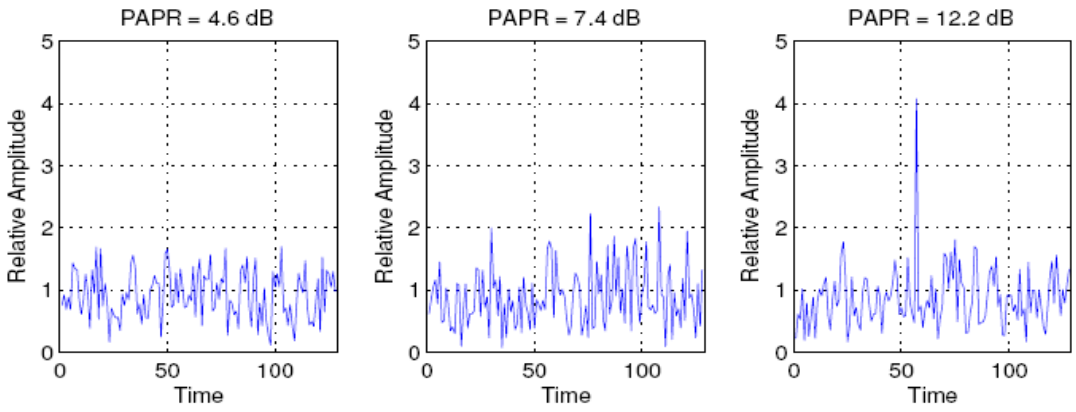

Figure 2.12: Three examples of OFDM symbols with 128 frequency bins and 64-QAM constellations scaled relative to the RMS amplitude. Depicted are a "typical" OFDM symbol (middle), as well as unusually "good" (left) and "bad" (right) symbols.

With the amplitude scaled down, most of the time the power amplifier is operating far from saturation. The efficiency of an amplifier is much lower when it is not near its maximum output value.

CHAPTER III

PAPR REDUCTION TECHNIQUES

3.1 PAPR Reduction

As it is mentioned previously, one drawback with OFDM is the high PAPR. This means that in the OFDM signal there is a large variation between the average signal power (Pav) and the maximum signal power (Pp). High PAPR will cause nonlinear distortion when the signal is applied to a transmitter which contains nonlinear component such as a power amplifier. Forcing the power amplifier to work in its linear region is one way to avoid such problem, but this technique is not power efficient. Another way to deal with the PAPR problem is to use some PAPR reduction method which means reducing the PAPR of the transmitted signal with some processing or manipulations of the OFDM signal itself before the power amplifier. There are different PAPR reduction techniques developed by processing the OFDM signal before the PA. This chapter is mainly focused on these PAPR reduction techniques.

3.2 Amplitude Clipping: Clipping is the simplest technique to reduce PAPR where peaks above a certain threshold, A_{max} are clipped. The clipped OFDM signal is represented as [1]

$$\hat{s}(t) = \begin{cases} s(t) & , |s(t)| \le A_{Max} \\ A_{Max} e^{j\Phi(s)} & , |s(t)| > A_{Max} \end{cases} \tag{26}$$

Where $\phi(s) = \arg[s(t)]$

Therefore, the magnitude of the clipped signal doesn't exceed A_{max}, and the phase of s(t) is preserved.

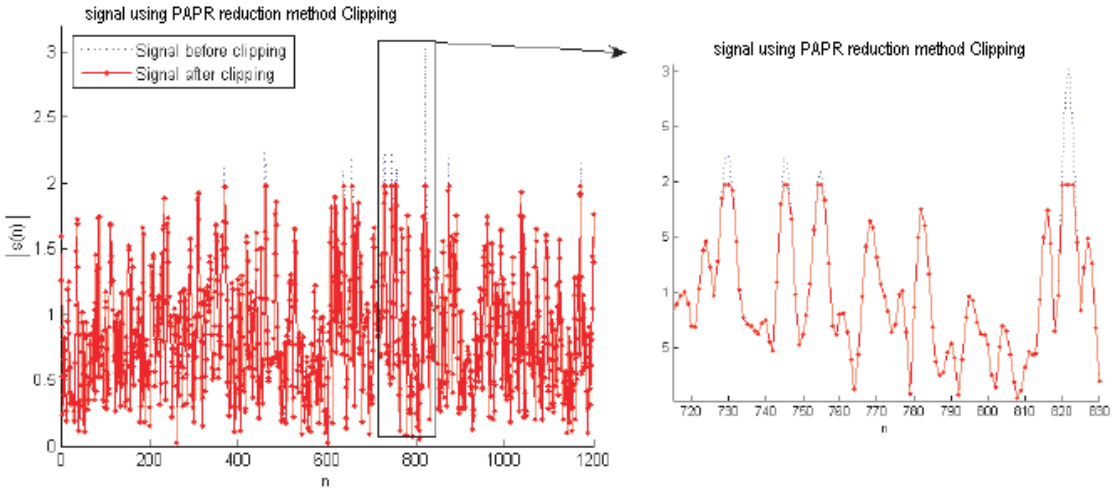

Figure 3.1: Operation of the clipping technique of a randomly generated baseband OFDM signal.

If A_{max} is very small, then significant spectral regrowth will occur. This phenomenon can be seen in fig. 3.2. Clipping an OFDM signal also introduces clipping noise which increases bit error rates (BER). Clipping noise can be thought of as approximately independent additive Gaussian noise [8], which leads to a simple symbol error rate (SER) expression in AWGN channel.

The signal to noise plus distortion ratio (SNDR) is defined as

$$SNDR = \frac{\sigma_s^2}{\sigma_N^2 + \sigma_C^2} \tag{27}$$

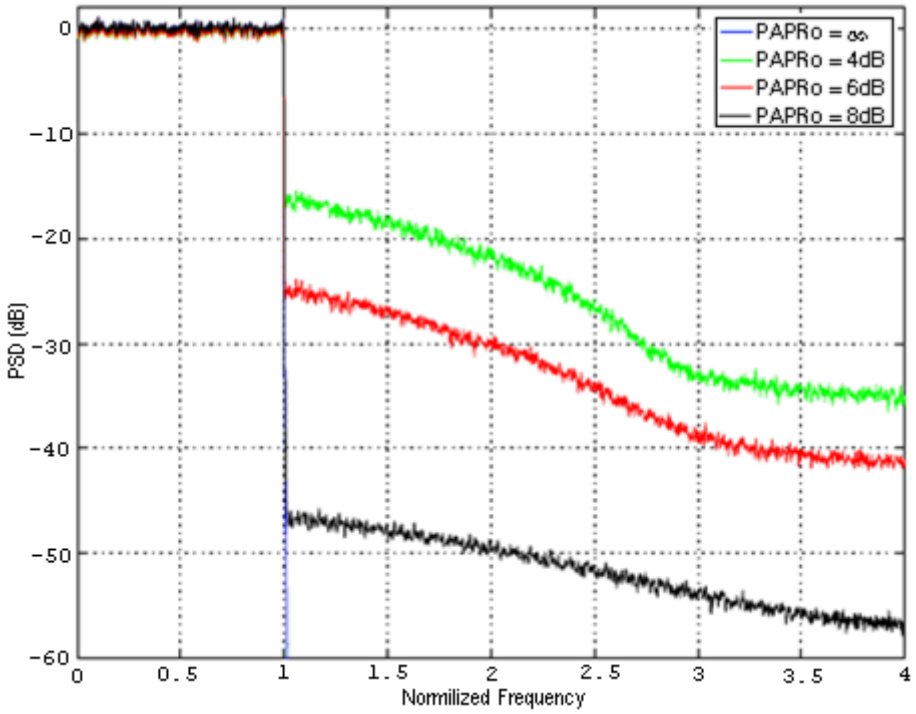

Figure 3.2: Power spectral density of clipped OFDM symbols where *N* = 1024. The unclipped case is presented along with clipping levels of {4; 6; 8} dB ($\sigma_s^2 = 1$).

The expected clipping noise power can be approximated as the tail expectation of a χ^2 distribution for large N because $s[n] \sim$ C.G.$(0, \sigma_s^2)$ *For* $PAPR_0 = \gamma$

$$\sigma_C^2 = \frac{1}{\sigma_s^2}\int_{\sigma_s^2\gamma^2}^{\infty} \gamma e^{-\gamma/\sigma_s^2} d\gamma \qquad (28)$$

$$= \frac{\left(1+\sigma_s^2\gamma^2\right)e^{-\sigma_s^2\gamma^2}}{\sigma_s^4}.$$

The symbol error rate (SER) for a QAM constellation for a clipped symbol in an AWGN channel can be approximated by [16]

$$SER = 1 - \left[1 - 2\left(1 - \frac{1}{\sqrt{M}}\right)Q\left(\sqrt{\frac{3SNDR}{M-1}}\right)\right]^2 , \qquad (29)$$

Where Q(.) is the tail area of the normal distribution. Figure 3.3 is a plot of the symbol error rate (SER) for different clipping levels. From the plot, it is seen that light clipping

(large γ) results in small increases in error rate.

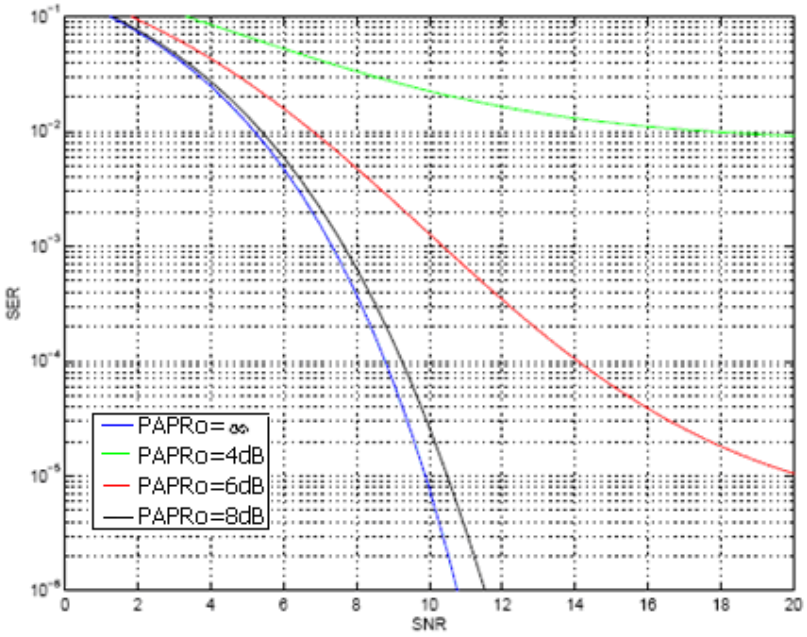

Figure 3.3: Approximate symbol error rate of clipped OFDM symbols for large *N* and *M* = 4. The unclipped case is presented along with clipping levels of {4; 6; 8} dB ($\sigma_s^2 = 1$).

Several techniques have been proposed to mitigate the spectral regrowth and SER increases due to clipping. Kim and Stuber in [9] present an iterative receiver design that tries to undo the clipping effect to increase the SER. The idea is to take the received clipped signal, and map it to constellation points so that an approximate frequency domain signal is generated. Then using the IDFT of the generated signal, an estimate of the unclipped signal can be found.

3.3 Companding:

In this technique, assume that the OFDM amplitudes are approximate Rayleigh distribution [10]. Companding is a composite word that combines **com**press and ex**pand.** The basic idea is to apply a compressing function, F(.), in the transmitter section and apply it to the OFDM symbol x so that F(x) is transmitted, where the range of F(x) is less than the range of x. Two companding functions are plotted in figure 3.4, the square root function and the μ-law function.

For this system, a μ-law companding technique is used. After companding the signal s(n), it becomes $s_c(n)$ [10]

$$S_c(n) = \frac{A.sign(s(n)).\ln\left[1+\mu\left|\frac{s(n)}{A}\right|\right]}{\ln(1+\mu)} \tag{30}$$

A is a normalization constant such that $0 \le \left|\frac{x(n)}{A}\right| \le 1$ and $\mu = \sqrt{(N-2)}$

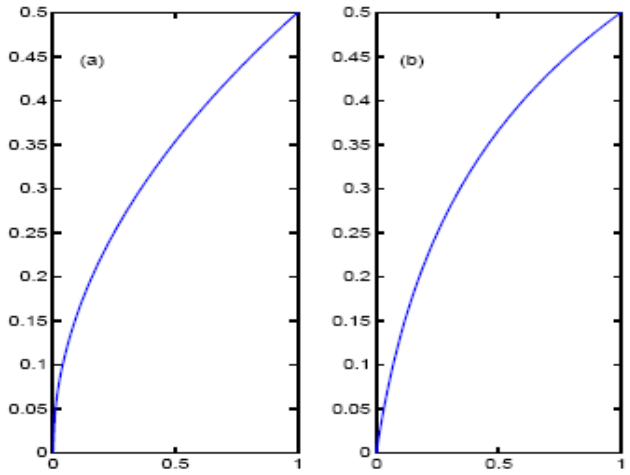

Figure 3.4: Two compressing functions. (a) is square root function, (b) is the μ-law function [10]

In the receiver section, the expanding function $F(.)^{-1}$ is applied to the receiver symbol so that $\hat{s} = F(s_c(n))^{-1}$ approximates the original symbol.

The expanding equation here is :

$$\hat{S}(n) = \frac{A.\exp\left[\frac{S_c(n)}{A.sign(S_c(n))}\ln(1+\mu)\right] - A}{sign(S_c(n)).\mu} \tag{31}$$

Figure 3.5 shows the waveforms of the OFDM signal before and after companding. It is seen that the amplitudes of small signals are enlarged while the peaks remain unchanged after companding. This shows that, the average power is increased and the peak-to-average power ratio is reduced.

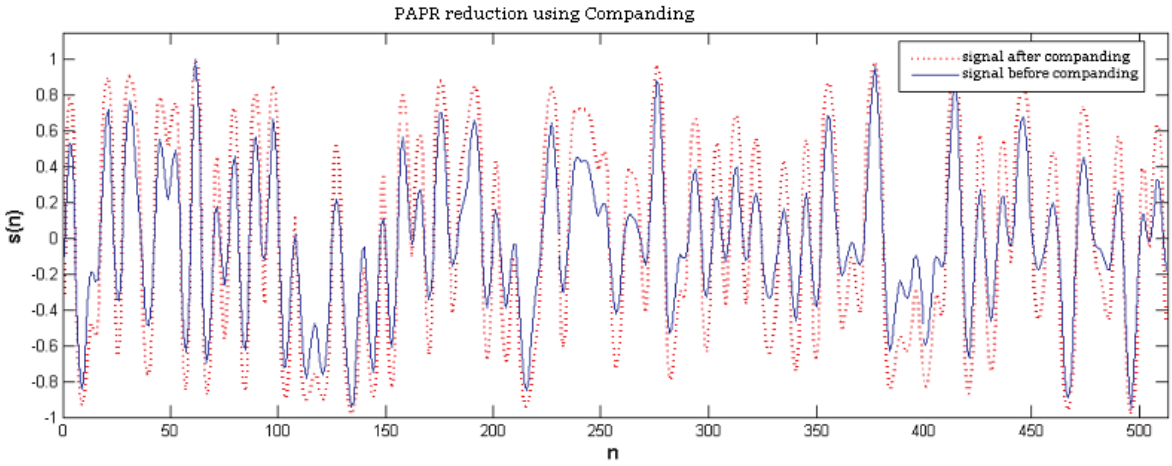

Figure 3.5: Operation of the companding technique of a randomly generated baseband OFDM signal.

3.4 Tone Reservation (TR)

This is an efficient technique to reduce the PAPR. There is no data distortion by using tone reservation. The basic idea is to reserve some OFDM subcarriers for PAPR reduction. These reserved subcarriers do not carry any data information. Instead, they are reserved for anti-peak signals. The aim is to find the time domain signal c (n) to be added to the original time domain signal $s_m(n)$ to cancel large peaks.

Figure 3.6 shows the operation of TR technique in discrete time domain. If we add the vector C (k) = F_d {c (n)} = $[C_0, C1, \ldots, C_{N-1}]^T$ to X_m (k) in the frequency domain, the new time domain signal can be represented as

$$\hat{S}_m(n) = s_m(n) + c(n)$$

$$= F_d^{-1}\{X_m(k) + C(k)\} \qquad (32)$$

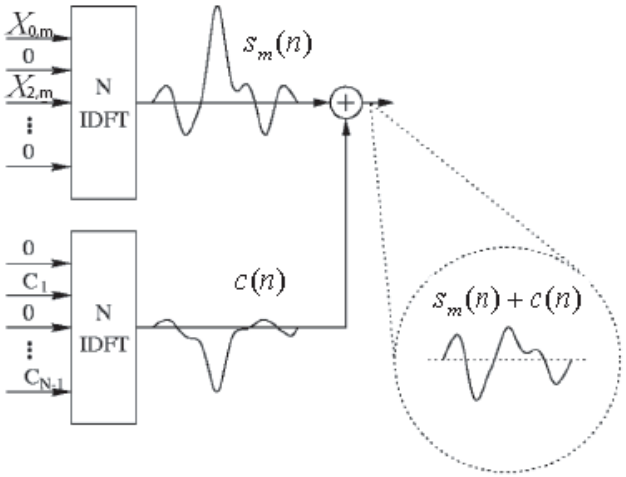

Figure 3.6: Operation of the tone reservation technique.

For baseband transmission, both s_m (n) and c (n) must be real therefore X_m (k) and C (k) must possess the Hermitian symmetry which mean $X_{k,m} = X^*_{N-k,m}$ and $C_k = C^*_{N-k}$ for even value of N. If N is odd similar constraints are necessary.

The new PAPR of the additive signal s_m (n) is defined as

$$PAPR = \frac{\max\left|\hat{s}_m(n)\right|^2}{E\left[\left|s_m(n)\right|^2\right]} = \frac{\max\left|s_m(n)+c(n)\right|^2}{E\left[\left|s_m(n)\right|^2\right]}, \quad where \quad E\left|c(n)\right| = 0 \qquad (33)$$

The TR technique restricts the data block X_m (k) and peak reduction vector C (k) to lie in disjoint frequency subspaces i.e. X_m (k)C (k) = 0. Let Γ= $\{i_q\}$ for q=1, 2, 3,…, L denote the vector of reserved tones in X_m (k), m=0, 1, 2,…, N-1 where L << N. then in the frequency domain we will have

$$X_m(k) + C(k) = \begin{cases} X_m(k) & ,k \in \Gamma^c \\ C(k) & ,k \in \Gamma \end{cases} \qquad (34)$$

Note that $X_{k,m} = 0$ when k $\epsilon\Gamma$ and $C_k = 0$ when k $\epsilon\Gamma^c$. The L nonzero value in C is called Peak Reduction Tones (PRT). To minimize the PAPR of s_m (n) + c (n) we must find a vector c (n), or equivalently C (k) that minimize [11]

$$\min_{c} \| s_m(n) + c(n) \|_\infty = \min_{C} \| s_m(n) + f_d^{-1}\{C(k)\} \|_\infty \quad (35)$$

Two algorithms to computing c (n) or C (k)) and reducing the PAPR of the OFDM signal will be presented in the following.

The first algorithm

The first one needs to compute IFFT more than one time for generation of anti-peak signal $\hat{c}(n)$ which may not be implemented in real system where the time is critic issue. For this algorithm assume that a PAPR value less than γ is wanted and there is a limit for number of iteration.

The algorithm:

1. Initial condition: m=0 and $\hat{s}_m(n)$ = s_m (n)
2. If PAPR $\leq \gamma$ jump to 9 where $\gamma = PAPR_o$
3. Clip s_m (n) to generate $s_m^{clip}(n)$
4. Compute $\hat{c}(n) = s_m^{clip}(n) - s_m$ (n)
5. Compute $\hat{C}(k) = F_d \{ \hat{c}(n) \}$
6. Set $\hat{C}(k) = 0$ for k $\epsilon\ \Gamma^c$
7. Compute $\hat{s}_m$ (n) = $F_d^{-1}\{ X_m (k) + \hat{C}(k) \}$
8. Increment the iteration counter, m = m + 1. if m< MaxIteration, Jump to 2.
9. Transmit $\hat{s}_m$ (n)

From now on, we cancel the index (n) from all the signals for simplicity and we assume Q = $F_d^{-1}\{\cdot\}$, where Q is the IDFT of size N*N, that is

$$Q = \frac{1}{\sqrt{N}} \begin{bmatrix} 1 & 1 & \cdots & 1 \\ 1 & e^{j\frac{2\pi}{N}1.1} & \cdots & e^{j\frac{2\pi}{N}1(N-1)} \\ \vdots & \vdots & \ddots & \vdots \\ 1 & e^{j\frac{2\pi}{N}(N-1).1} & \cdots & e^{j\frac{2\pi}{N}(N-1)(N-1)} \end{bmatrix}_{N\times N} \quad (36)$$

The description here strictly follows Tellado's description in [11].

The second algorithm

The second algorithm [from 11] is based on taking the gradient of the Mean Square Error (MSE) of the transmitter distortion function. The idea of the gradient algorithm comes from clipping. By taking the gradient of the clipping noise MSE, the PAPR will be reduced after a few steps. Let's call $\hat{C}$ the vector of length L obtained by selecting the nonzero value from C, i.e. $\hat{C}$ = [C_{i1} ,C_{i2} , · · · ,C_{iL}], and similarly $\hat{Q}$ the submatrix of Q constructed by choosing its columns {i_1, i_2, . . . , i_L}, i.e. $\hat{Q}$ = [q_{i1} |q_{i2} | · · · |q_{iL}]. Then

$$c = QC = \hat{Q}\hat{C} \tag{37}$$

since the remaining values of C are zero. Using 41, the general additive PAPR reduction expression in 36 can be simplified to

$$\hat{s}_m = s_m + c = s_m + QC = s_m + \hat{Q}\hat{C} \tag{38}$$

This algorithm begin by clipping the signal and the clipper is defined as

$$clip \quad A(s_{k,m}) = \begin{cases} s_{k,m} & , \ |s_{k,m}| \le A \\ Asign(s_{k,m}) & , \ |s_{k,m}| > A \end{cases} \tag{39}$$

then the clipping noise power of the transmitted sequence s_m, is

$$\left\| s_m - clipA(s_m) \right\|_2^2 = \sum_{n=0}^{N-1} (s_{n,m} - clipA(s_{n,m}))^2 \tag{40}$$

and the Signal to Clipping noise Ratio (SCR) will be

$$SCR = \frac{\left\| s_m \right\|_2^2}{\left\| s_m - clipA(s_m) \right\|_2^2} \tag{41}$$

If we include the PRT to these equations, the transmitted sequence is s_m + c and the SCR is

$$SCR = \frac{\left\| s_m \right\|_2^2}{\left\| s_m + c - clipA(s_m + c) \right\|_2^2} \tag{42}$$

Now to maximize SCR, the denominator of (46) must be minimized. In [11] shows that the gradient of the denominator of (46) with respect to $\hat{C}$ is

$$\nabla_{\hat{C}\|s_m+c-clipA(s_m+c)\|_2^2} = \sum_{|s_{i,m}+c_i|>A} sign(s_{i,m}+c_i)(|s_{i,m}+c_i|-A)\hat{Q}\,\hat{q}_{row}^{\,i} \quad (43)$$

where A is the clipping level and $\hat{q}^{i}_{row}$ denotes the i [th] row of $\hat{Q}$.

The algorithm:

1. Initial condition: set $\hat{s}^{0}_{m} = s_{m.}$

2. Peak detection: Find the OFDM symbol samples n for which $|\hat{s}_{n,m}| > A$. If all samples are below the target A, jump to 5.

3. Update $\hat{s}^{i}_{m}$ according to

$$s_m^{k+1} = s_m^k - \mu \sum_{|s_{n,m}+c_n^{(k)}|>A} \alpha_n^{(k)} p^0[(n-m)_N] \quad (44)$$

4. Increment the iteration counter, i = i + 1. if i < MaxIteration, Jump to 2.

5. Transmit $\hat{s}^{i}_{m.}$

Because in the TR technique L carriers will be reserved for anti peak signals therefore the systems total data rate will decrease.

3.5 Tone Injection

Motivated by the data rate loss of tone reservation, Tellado introduced another technique known as tone injection [11]. In tone injection, the constellation is enlarged to include *S* times as many points as the original constellation. The extra constellation points are generated by shifting copies of the original constellation. Figure 3.7 illustrates the possible positions for a QPSK constellation for tone injection when *S* = 9. That is, there are 8 alternative representations for each constellation point. If necessary, *S* could be made larger by extending the replication pattern over more of the signal plane. The constellations are separated by distance *p* where for an M-QAM constellation $p \geq d_{\min} \log_2 M$ so that $d_{\min}$ for the extended constellation is the same as the original $d_{\min.}$

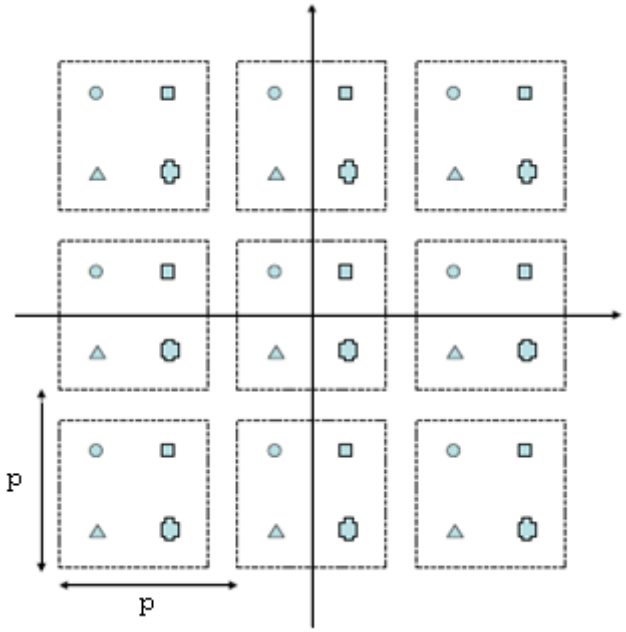

Figure 3.7: QPSK constellation extended for tone injection (*S* = 8).

Tone injection works by moving constellation points from the original constellation to one of its corresponding points in the extended constellation. If done properly, this rearrangement will lead to a PAPR reduction. The clever trick is that the receiver can recover which constellation point a received extended point corresponds to by taking the modulo *p* of the in-phase and quadrature-phase components of the received signal. Thus, no side information is necessary to recover the original signal from the PAR reduced signal. However, it is obvious that any extension of the constellation will increase the average power.

3.6 Partial Transmit Sequence (PTS)

Partial Transmit Technique is one popular technique to reduce the peak-to-average power ratio (PAPR) in OFDM systems. In PTS, non-overlapping subsets of OFDM subcarriers are formed, rotated independently, and combined again. Since signal representations corresponding to different rotations results in different PAPR, selecting the representation with the minimum PAPR leads to PAPR reduction.

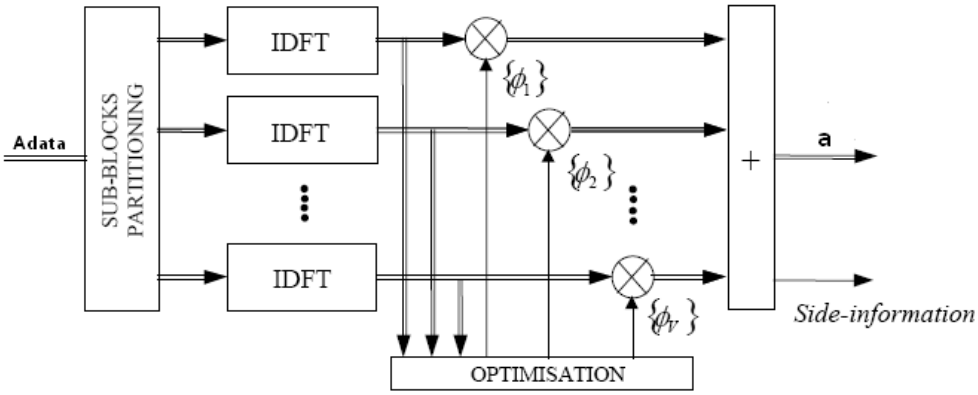

Figure 3.8 : Partial Transmit Sequence scheme

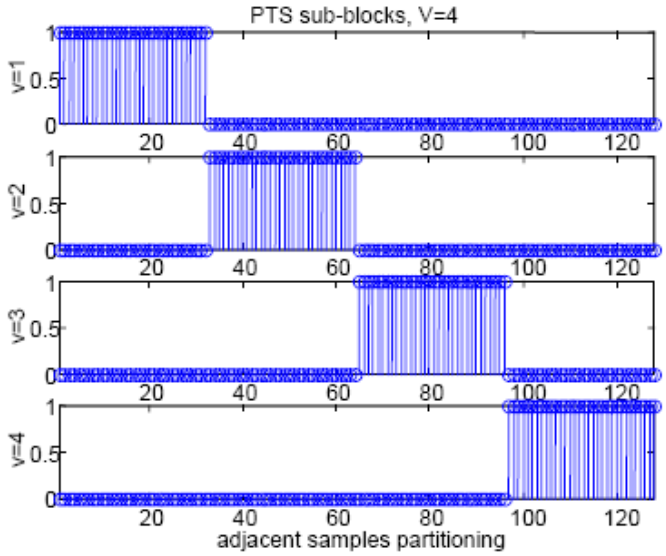

Figure 3.9: Example of partitioning of a symbol into sub-blocks for the application of PTS technique

In PTS, the data symbols in A are partitioned into V disjoint subblocks $A^{(v)} = [A_0^{(v)},..., A_{N-1}^{(v)}]$ with $A_k^{(v)} = A_k$ or 0, $0 \le v \le V-1$, such that

$$A = \sum_{v=0}^{V-1} A^{(v)} \tag{45}$$

The subblocks $A^{(v)}$ are transformed in to V time domain partial transmit sequences.

$$a^{(v)} = [a_0^{(v)}, \cdots, a_{N-1}^{(v)}] = IDFT\ (A^{(v)}) \tag{46}$$

These sequences are independently rotated by some phase factors $b_v = e^{j\varphi_v}$ and then combined to produce the time-domain OFDM signal.

$$a = \sum_{v=0}^{V-1} b_v a^{(v)} \tag{47}$$

Assuming that φ_v and thus b_v can attain W different values there are W^V alternative representations for an OFDM symbol. These representations correspond to all the possible vectors $b = [b_0, b_1, b_2 \cdots, b_{V-1}]$. Partial transmit technique selects a vector $\hat{b}$ such that the PAPR of the corresponding transmit sequence $\hat{a}$ is the minimum among all different sequences. Then sequence with this minimum PAPR is transmitted.The side information that needs to be transmitted to inform the receiver about the selected vector is $R = V \log_2 W$ bits. This scheme is complex compared to other techniques as it requires a bank of IFFT operations.

3.7 Selected Mapping Scheme (SLM)

A relatively simple approach to generate the different versions of the same symbol is that of phase-rotating the symbol to be transmitted in different ways. This technique was proposed by Bauml and etal [21].

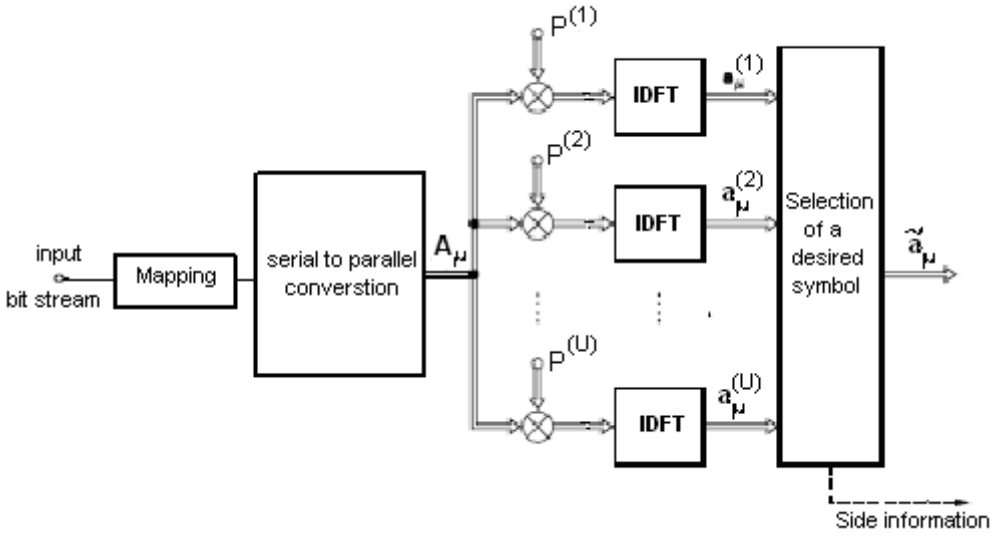

Figure 3.10 : Selected mapping scheme

As seen in this scheme, such a system requires the replication of modulation operation, specifically the IFFT, a number of times equal to the chosen number of alternate transmit sequences to be generated. A variant of the signal is input to the block that executes the Fourier transform, already mapped in its in-phase and

quadrature components. Phase rotation of constellations is conceptually equivalent to operating a statistical selection of those mappings that are best suited to transmission, hence the name Selected Mapping. By properly selecting the phase sequences, the output modulated symbols will be different and can be considered statistically independent, and the transmitter can choose to send the one with minimum peak.

3.8 Comparison of main PAPR reduction techniques

The table below compares the 6 main PAPR reduction techniques based on side information, data rate reduction, BER increase and complexity. In fact PAPR reduction is achieved for these different techniques at the expense of distortion of the original signal, power increase, bandwidth efficiency decrease, bit error rate (BER) increase, data rate loss, side information needed, computational complexity increase, etc. Depending on the devices used in the multi carrier transmission systems like digital to analogue (D/A) converter, and power amplifier (PA) we have to choose the PAPR reduction technique very carefully. There is no specific PAPR reduction technique that that is best for all multicarrier systems.

Techniques	PAPR reduction	BER increase	Data rate loss	Side information needed	Computational Complexity
Clipping	yes	Yes	No	No	less
Companding	Better compared to clipping	Yes	Yes	No	Less complex
Tone Reservation (TR)	Better than Companding and Clipping	No (no distortion of original signal)	Yes	No	High (multiple iteration operations after IFFT)
Tone Injection (TI)	Same as TR	No	No	No	High (comparable with TR)
PTS	Very good Compared to others	No	No	Yes	High
Selected Mapping	Very good Similar with PTS	No	No	Yes	high

Based on the above comparison, it is found that selected mapping and PTS are the most effective candidates for PAPR reduction up to the desired level. (In fact, none can achieve 0dB PAPR). Both Selected Mapping and Partial transmit Sequences are capable of improving the statistical characteristic of the OFDM PAPR by allowing little additional redundancy. Selected Mapping is more advantageous, if the amount of redundancy for side information is concerned. Both have almost equal performances in all other aspects. Thus the next chapters focus mainly on Selected mapping PAPR reduction technique. A modified (or enhanced) method of Selected Mapping is presented to facilitate the implementation of the highly promising modulation method OFDM for on going high data rate digital transmission applications.

CHAPTER IV

ENHANCED SELECTED MAPPING TECHNIQUE

4.1 Conventional Selected Mapping

Peak to average power ratio (PAPR) reduction using Selected Mapping (SLM) is first introduced by R. W. Bauml and etal in [21]. But, the idea of mapping a signal to different and equivalent signal representations is very general and has been applied in several different forms for OFDM. One such scheme was shown in [38], where a method based on selected clipping was introduced. The idea was to create different signal representations of an OFDM symbol, the signals are statistically independent alternative transmit sequences representing the same information. Then the sequence with the lowest PAPR is selected for transmission.

The PAPR of an OFDM signal is very sensitive to phase shifts in the frequency-domain data and selected mapping is based on this effect of phase shift. PAPR reduction is achieved by multiplying independent phase sequences by the original OFDM data and determining the PAPR of each phase sequence/data combination. The sequence/data combination with the lowest PAPR is transmitted. The effectiveness of selected mapping technique basically depends on the number of generated phase sequences. If $\boldsymbol{X}$ is the data sequence, $\boldsymbol{X}$ is element-wise phased by U N-length phase sequences, $\left\{\Phi[k]^{(u)}\right\}_{k=0}^{N-1} = \Phi^{(u)}$ where u is an integer such that $u \in [0, U - 1]$; k=0, 1, 2,…, N-1 and N is length of data.

After phasing, the U different frequency-domain sequences are given by

$$\boldsymbol{X}^{(u)} = \boldsymbol{X} \, o \, e^{j\Phi^{(u)}} \tag{48}$$

Where o is element-wise multiplication and set $\Phi^{(0)} = 0$ so that $\boldsymbol{X}^{(0)} = \mathbf{X}$ (original OFDM data). In time domain, define the U OFDM symbols $x^{(u)} = IDFT\left\{X^{(u)}\right\}$

Note that U symbols carry the same information. So for PAPR reduction to be achieved, the symbol with minimum PAPR is transmitted.

Define

$$\tilde{u} = \arg\min_{0 \le u < U} \; PAPR\left\{x^{(u)}\right\} \tag{49}$$

4.2 Recovery of data at receiver

The data is recovered at the receiver side by employing a DFT operation. With $\tilde{u}$ the transmitted signal is $x^{(\tilde{u})}$, At the receiver,

$$X = DFT\left\{x^{(\tilde{u})}\right\} \circ e^{-j\Phi^{(u)}} \tag{50}$$

$$= X \circ e^{j\Phi^{(u)}} \circ e^{-j\Phi^{(u)}}$$

$$= X$$

the receiver has to know all $\Phi^{(u)}$ to recover x. i.e. the receiver has to know what has been done at the transmitter through transmission of $\lceil log_2 U \rceil$ bit of side information. The transmission of side information is particularly critical in this technique, since decoding error in this case would lead to a high risk of interpreting the whole data symbol in a wrong way, it is thus important to protect side information by sending it with proper protection which reduces the probability of error.

4.3 PAPR calculation using Selected Mapping

As is detailed in chapter 2, the distribution of PAPR values for OFDM signals is expressed in terms of Complementary cumulative distribution function (CCDF). Selected Mapping PAPR reduction scheme creates U independent mappings of discrete-time domain signal x. By making the assumption that each mapping is independent of all other mappings, the CCDF of the PAPR in a selected mapping scheme is

$$\Pr\left[PAPR\left\{x^{(u)}\right\} > PAPR_0\right] = \Pr\left[\bigcap_{u=0}^{U-1}\left(PAPR\left\{x^{(u)}\right\} > PAPR_0\right)\right], u \in [0, U\text{-}1] \tag{51}$$

$$= \Pr\left[PAPR\{x\} > PAPR_0\right]^U$$

It is shown in equation (20) that

$\Pr\left[PAPR\{x\} > PAPR_0\right] = \left(1 - e^{-PAPR_0}\right)^N$. Substituting this in to equation (61), we get

$$\Pr\left[PAPR\left\{x^{(u)}\right\} > PAPR_0\right] = \left[1 - \left(1 - e^{-PAPR_0}\right)^N\right]^U \tag{52}$$

Or

$$CCDF = \left[1-\left(1-e^{-PAPR_0}\right)^N\right]^U$$

Because of the varying assignments of data to the transmit signal, it is so named as Selected Mapping (SLM). U statistically independent OFDM frames represent the same information. Selecting the frame with the lowest PAPR for transmission, the probability that $PAPR_{low}$ exceeds the threshold value $PAPR_0=\gamma$ is given by

$$CCDF = \left[1-\left(1-e^{-\gamma}\right)^N\right]^U \qquad (53)$$

Figure 4.1 shows the theoretical PAPR CCDF curves for OFDM symbol for $N = 2^k$, k=5, 6, 7, 8 and U=5.

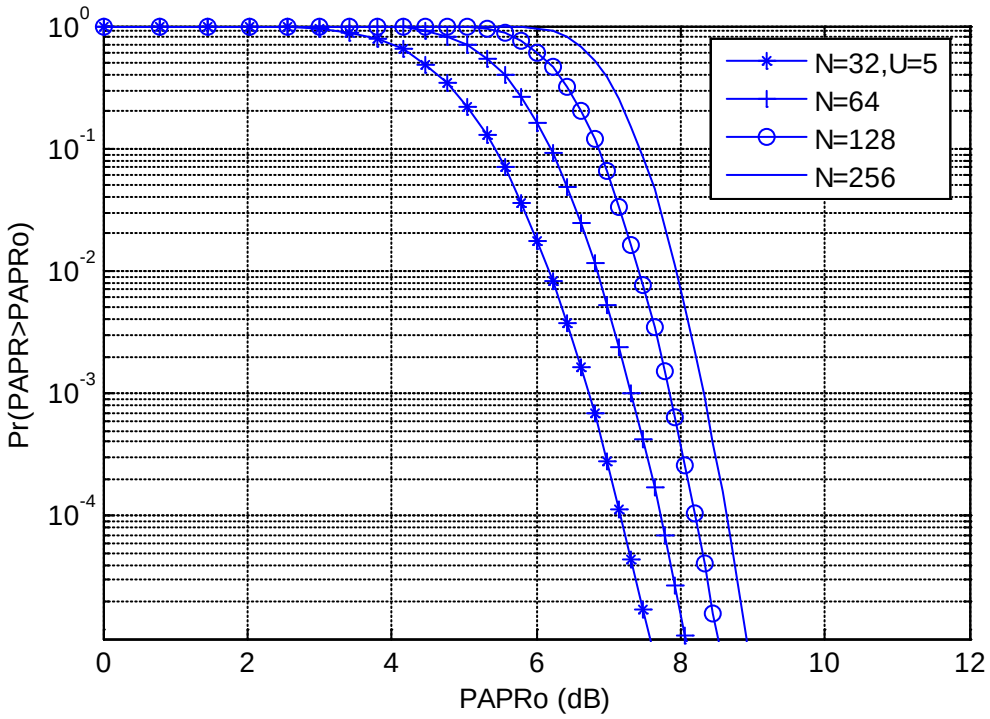

Figure:4.1 Theoretical PAPR CCDF of OFDM for N=32, 64, 128, 256 and U=5.

From the plot, one can see that PAPR increases with increase of N and large PAPR reduction is possible with selected mapping. Figure 4.2 shows the effect of increasing phase sequences (U) up on PAPR for N=64, U=2, 8, 32, and 100.

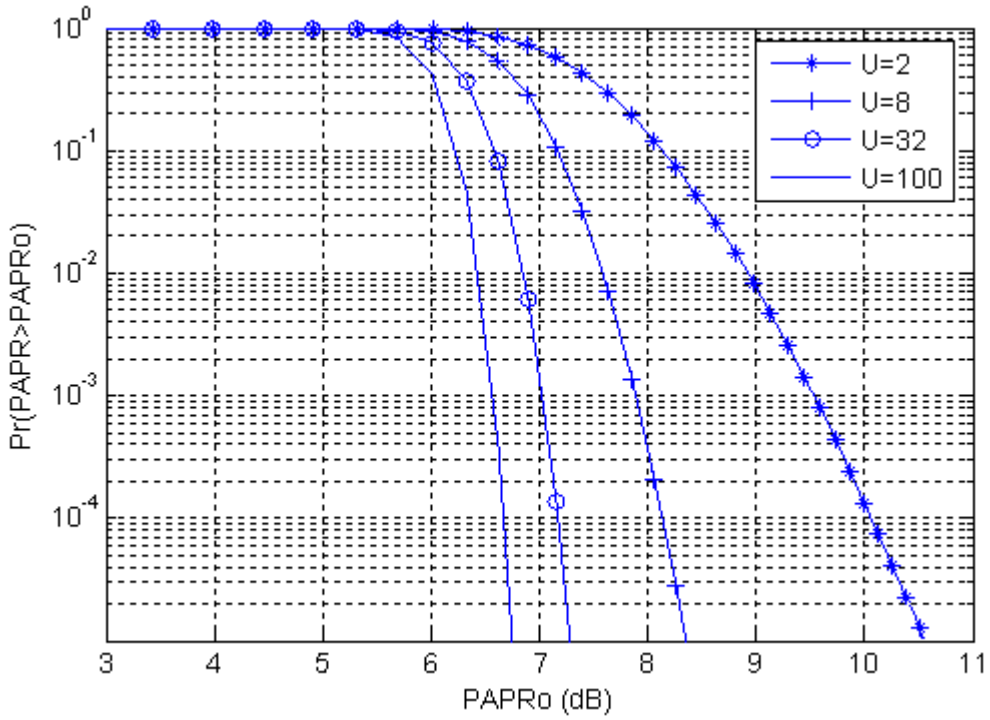

Figure:4.2 Theoretical PAPR CCDF of OFDM for N= 64, and U=2, 8, 32, 100

The computational complexity of this scheme increases as the number of phase sequences U increases as it requires U IFFT processors. The computational complexity is measured by the number of complex additions and complex multiplications performed in the IFFT processor. It is this computational complexity that limits its implementation.

4.4 Generation of OFDM frames representing the same information

Define U different vectors $P^{(u)} = \left[p_1^{(u)}, \cdots, p_N^{(u)} \right]$,

With $p_\mu^{(u)} = e^{j\varphi_\mu^{(u)}}$, $\varphi_\mu^{(u)} \in [0, 2\pi)$, $\mu = 1:N$, $u = 1:U$. For example, if we take $\varphi \in \{ 0, \pi/2, \pi, 3\pi/2 \}$, $P_\mu \in \{\pm 1, \pm j\}$. Then we can choose randomly a phase sequence P_μ =[1,j,-1,-j, 1,j,-1,-j, 1,j,-1,-j, 1,j,-1,-j,…,] as one possible phase sequence. After mapping the information on the carriers to the carrier amplitudes A μ , each OFDM frame is multiplied carrierwise with the U vectors $P^{(u)}$, resulting in a set

of U different frames all representing the same information. For this case, A μ is taken as unit magnitude.

$$A^{(u)}[\mu] = A[\mu].e^{j\varphi_{\mu}^{(u)}}, \quad \mu = 1:N \quad u = 1:U \tag{54}$$

Then all U frames are transformed in to time domain and one with the lowest PAPR is selected for transmission.

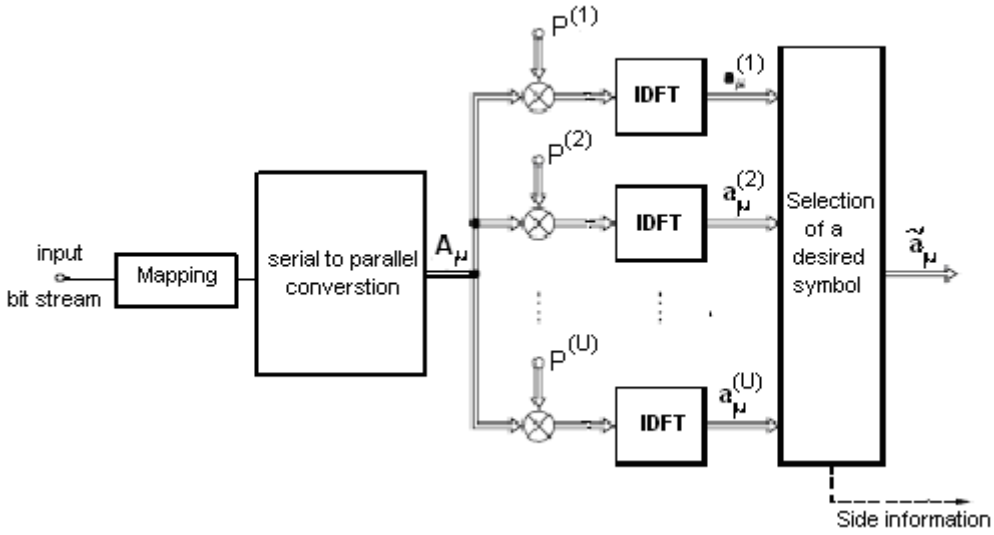

Figure: 4.3 PAPR reduction with selected mapping

The phase sequences, P(n) are generated randomly with $p_{\mu}^{(n)} \in \{\pm 1\}$. The advantage of using this phase shifts is that they can be implemented without any complex multiplications.

Selected mapping technique improves PAPR statistics of an OFDM signal significantly without any in-band distortion and out-of-band radiation. To detect the

OFDM signal at the receiver, appropriate side information indicating how the transmitter generates the output signal is embedded in the transmitted signal with error control codes for protection.

There are other approaches that do not require the transmission of side information. In one technique, a part of the subcarriers are used as peak reduction subcarriers and the value (amplitude and phase) of the peak reduction subcarriers are varied such that the resulting OFDM signal has lower PAPR. At the receiver, the information on the peak

reduction subcarriers is simply ignored. But in this technique, a portion of subcarriers should be allocated as peak reduction subcarriers, resulting in a data rate loss.

The computational complexity of selected mapping is high as it requires a bank of IFFTs to generate a set of candidate signals. One technique developed in [39] to reduce the computational complexity is thresholding the PAPR in selected mapping. Threshold selected mapping is based on calculating the maximum number of phase sequences (U) instead of taking random number of U. This is made by keeping the probability of clipping at an acceptable level.

4.5 Enhanced Selected Mapping

It is mainly the increase of this computational complexity that restricts the implementation of conventional SLM for the OFDM system with large carriers. The computational complexity of the conventional selected mapping is increased in proportion to the number of phase sequences (U), simply because the alternative input symbol sequences that should be individually IFFTed for PAPR comparison are generated at the initial stage of IFFT. Now, if the computational complexity depends on the number of phase sequences generated at the initial stage of IFFT, what will happen if the phase sequences are generated at some intermediate stage of IFFT not at the initial stage, so that the computational complexity is mitigated?

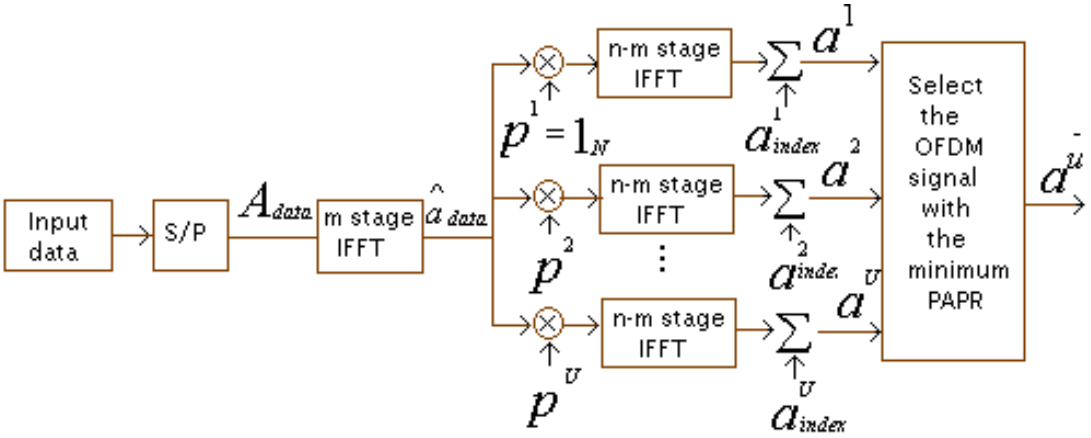

Figure 4.4 Block diagram of the enhanced selected mapping scheme

In the previous selected mapping scheme, alternative transmit symbol sequences $A^U = [A_0^u, A_1^u, \cdots, A_{N-1}^u]$, $1 \le u \le U$ are obtained by multiplying the phase

sequences $P^U = [P_0^u, P_1^u, \cdots, P_{N-1}^u]$, $1 \le u \le U$ to the input symbol sequence $A = [A_0, A_1, \cdots, A_{N-1}]$. By component-wise multiplication, $A_n^u = A_n P_n^u$, $0 \le n \le N-1$. To preserve power, unit magnitude is assigned to each symbol of the phase sequences. For simplicity purpose, P_n^u will be selected from {±1}. Finally, the OFDM signal with $a^u = IFFT\{A^u\}$ having the smallest PAPR is selected for transmission. This was the conventional selected mapping technique.

Here in the modified technique, the different phase sequences are multiplied to the intermediate signal, which is the partially IFFTed input symbol sequence.

Fig. 4.4 shows the block diagram of the enhanced selected mapping scheme. In this scheme, the N (= 2^n) point IFFT based on decimation-in-time algorithm is partitioned into two parts. The first part is the first m-stages of IFFT, and the second part is the remaining n-m stages. A set of OFDM signals is generated by multiplying different phase sequences P^u , $1 \le u \le U$ by the intermediate signal $\hat{\mathbf{a}}_{\mathbf{data}}$ after the mth stage of IFFT. If we compared this enhanced technique to the previous selected mapping scheme, the computational complexity of this scheme is much less as the intermediate signal $\hat{\mathbf{a}}_{\mathbf{data}}$ is used in common. To provide the receiver with the information on the phase sequence, an index symbol sequence $\mathbf{A}_{\mathbf{index}}$ containing this information is added to the data symbol sequence $\mathbf{A}_{\mathbf{data}}$ to form the input symbol sequence $\mathbf{A}$, i.e., $\mathbf{A}=\mathbf{A}_{\mathbf{data}}+\mathbf{A}_{\mathbf{index}}$. The index information is encoded for error detection and correction purpose. For M-QAM modulation, with encoder code rate R and number of phase sequences U, the number of index symbols we need to transmit is $\lceil \log_M U/R \rceil$, where $\lceil y \rceil$ denotes the smallest integer exceeding or equal to *y*. To reserve this index information, $\lceil \log_M U/R \rceil$ elements of $\mathbf{A}_{\mathbf{data}}$ are set to zero and N-$\lceil \log_M U/R \rceil$ elements of $\mathbf{A}_{\mathbf{index}}$ are set to zero. This index information is then stored in the memory. Therefore, if the index signal a_{index}^u is added after IFFT of A_{index}^u, we can write the enhanced selected mapping OFDM signal a^u as

$$a^u = IFFT_{m+1}^{n}\left\{P^u \otimes IFFT_1^m\left(A_{data}\right)\right\} + IFFT_1^n\left\{A_{index}^u\right\}$$
$$= IFFT_{m+1}^{n}\left\{P^u \otimes \hat{a}_{data}\right\} + a_{index}^u \qquad (55)$$

where $IFFT_m^n$ indicates IFFT from m stage to n stage, and the size of IFFT is $N=2^n$.

4.6 Phase Sequences of enhanced SLM Scheme

As in the conventional SLM OFDM scheme, we put the restriction on the phase sequences to be {±1} sequences and the phase sequence can be randomly selected from {±1}. A simple technique of using a random sequence of {±1} is to use the rows of a Hadamard matrix.

4.7 Hadamard Matrix

A (±1)-matrix is a matrix whose entries are 1 and -1. An n x n (±1)-matrix is called an Hadamard matrix if the rows and columns are orthogonal and satisfies $HH^T = nI$.

There are two reasons why we use the rows of a cyclic Hadamard matrix. The first reason is because they themselves are good candidates for phase sequences in the conventional SLM scheme [21], and the second is because the numerical analysis shows that there is only a negligible performance degradation when we extend the rows of a cyclic Hadamard matrix H_2^{n-k} by repeating 2^k times and use them as phase sequences [21].

4.8 Computational Complexity

It is shown in next chapter that SLM has significant PAPR reduction capabilities. However, this reduction is not free. The most significant costs are the *U*- 1 additional IDFT operations, and the *U*- 1 *N*-length phase multiplications. These complexities can be mitigated slightly by using the inverse fast Fourier transform (IFFT) in place of the IDFT and by using binary phase sequences so that all of the phase multiplications are just sign changes.

The enhanced Selected Mapping technique indicated here in this thesis reduces the computational complexity of conventional Selected Mapping to a level that can easily be implemented in practical OFDM applications. Recall that the IFFT algorithm works by using $n = \log_2 N$ stages of radix-2 decimation of the input sequence *X*. Let us denote the output after the m^{th} stage by $IFFT^{(m)}\{X\}$. By generating an intermediate IFFT of the data sequence, $IFFT^{(mo)}\{X\}$, and phasing this sequence by phase vectors, we can

create $IFFT^{(mo)}\{X\}$ o $e^{j\phi^{(u)}}$. This is a reduction in complexity because only $n - m_o$ IFFT stages need to be calculated in order to determine the PAPR of each sequence. Mathematically, the candidate sequences in this scheme are

$$x^{(u)} = IFFT^{(n-m_o)}[IFFT^{m_0}\{X\} \circ e^{j\phi^{(u)}}]. \quad (56)$$

These results show that for $N = 2^{11}$=2048, if $m_o = 5$,U=16 the computational complexity savings of 51% is achieved without a noticeable reduction in PAPR performance.

Let's calculate the computational complexity for both the conventional and the enhanced Selected Mapping schemes by comparing the number of multiplication and addition involved in each case.

When the number of carriers is $N=2^n$, the numbers of complex multiplication n_{mul} and complex addition n_{add} of the conventional selected mapping OFDM scheme are given by $n_{mul}=2^{n-1}nU$ and $n_{add}= 2^nnU$, where U is the total number of phase sequences.

If the phase sequences are multiplied after the m^{th} stage of IFFT (for enhanced scheme), the numbers of complex computations of the enhanced selected mapping scheme are given by $n_{mul}=2^{n-1}n+2^{n-1}(n-m)(U-1)$ and $n_{add}= 2^nn+2^n(n-m)(U-1)$.

The computational complexity reduction is evaluated in terms of computational complexity reduction ratio (CCRR) of the enhanced selected mapping scheme over the conventional selected mapping OFDM scheme is defined as

$$CCRR = \frac{complexity\ \ of\ \ conventional\ \ SLM - complexity\ \ of\ \ enhanced\ \ SLM}{complexity\ \ of\ \ conventional\ \ SLM} \times 100$$

$$CCRR = \left(1 - \frac{Complexity\ of\ enhanced\ SLM}{Complexity\ of\ conventional\ SLM}\right) \times 100$$

Complexity of conventional SLM=number of complex additions + number of complex multiplications

$$=2^{n-1}nU + 2^nnU$$

Complexity of enhanced SLM=$2^{n-1}n+2^{n-1}(n-m)(U-1) + 2^nn+2^n(n-m)(U-1)$

Simplifying we get,

$$CCRR = \left(1 - \frac{1}{U}\right)\frac{m}{n} \times 100 \quad (57)$$

Table I gives the CCRR of the enhanced selected mapping scheme over the conventional selected mapping scheme with typical given values of U, m and n

Table I

CCRR of modified selected mapping scheme over the conventional selected mapping scheme

n-m	CCRR (%)									
	N=128(n=7)		N=256 (n=8)		N=512 (n=9)		N=1024(n=10)		N=2048 (n=11)	
	U=4	U=8	U=4	U=8	U=4	U=8	U=4	U=8	U=4	U=8
4	32	38	38	44	42	49	45	53	48	56
5	21	25	28	33	33	39	38	44	41	48
6	11	13	19	22	25	29	30	35	34	40

We can observe from the table that more complexity reduction is obtained when n-m is less. i.e., when m is near n or when the m^{th} IFFT stage is near the final stage.

For instance, when N=2048 $=2^{11}$ and n-m = 5, and U=16, 51% computational complexity savings is achieved. This can be directly related to the OFDM processor or execution time. For instance, a HI PAR DSP4 2048 point FFT/IFFT processor has 222μsec execution time. When n-m=5, we require a 32 point processor and the execution time will be around 0.4μsec. Thus much processing time is saved through the enhanced Selected Mapping technique developed in this thesis and implementation will be simple.

To avoid the performance degradation due to channel, channel coding is usually used in communication systems.

CHAPTER V

SIMULATION, RESULTS, AND DISCUSSIONS

In this chapter, we will discuss the Matlab simulation performed for the OFDM DVB-T system of the IEEE standard 802.16 [28] intended for mobile reception of digital TV. The OFDM system specified in this system (2K mode DVB-T) has 2048 carriers with QPSK, 4QAM, and 16QAM constellation. The number of used carriers is 1705. The remaining 343 carriers are set to zero to shape the power spectral density of the transmit signal. 50 000 input symbol sequences are generated randomly with uniform distribution. Detail analysis of this system is found in appendix B.

Numerical values for the OFDM parameters used are listed in the table below.

Table 2: OFDM parameter values

Parameter	**Value**			
Elementary period T	7/64μs			
Number of carriers	1,705			
Value of carrier number K_{min}	0			
Value of carrier number K_{max}	1704			
Duration T_u	224μs			
Carrier spacing 1/ T_u	4,464 Hz			
Spacing between carriers K_{min} and k_{max}(K-1)/ T_u	7.61 MHz			
Allowed Guard interval Δ/T_u	1/4	1/8	1/16	1/32
Duration of symbol part T_u	2,048×T=224 μs			
Duration of Guard interval Δ	512×T 56 μs	256×T 28 μs	128×T 14 μs	64×T 7 μs
Symbol Duration T_s=$\Delta + T_u$	2,560×T 280 μs	2,304×T 252 μs	2,176×T 238 μs	2,112×T 231 μs

5.1 Conventional Selected Mapping Simulation Model

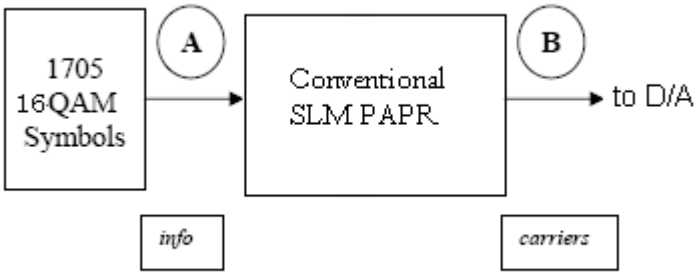

Figure: 5.1: OFDM symbol generation using conventional SLM.

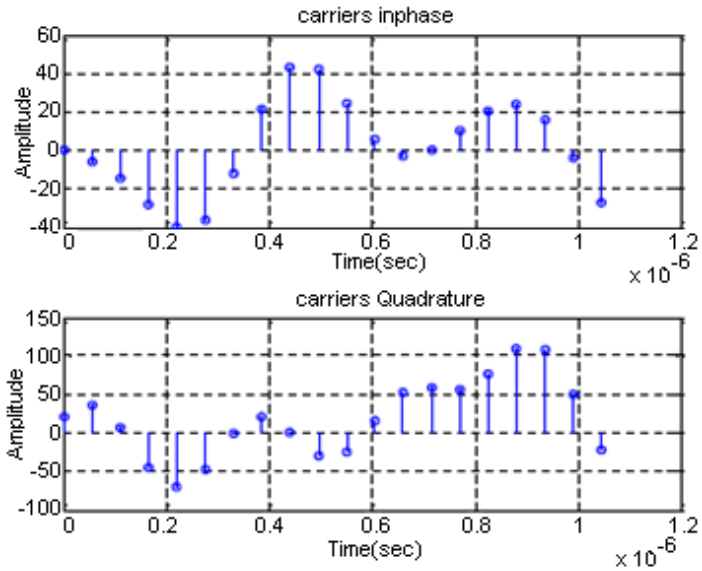

Figure 5.2: Time response of signal carriers at B

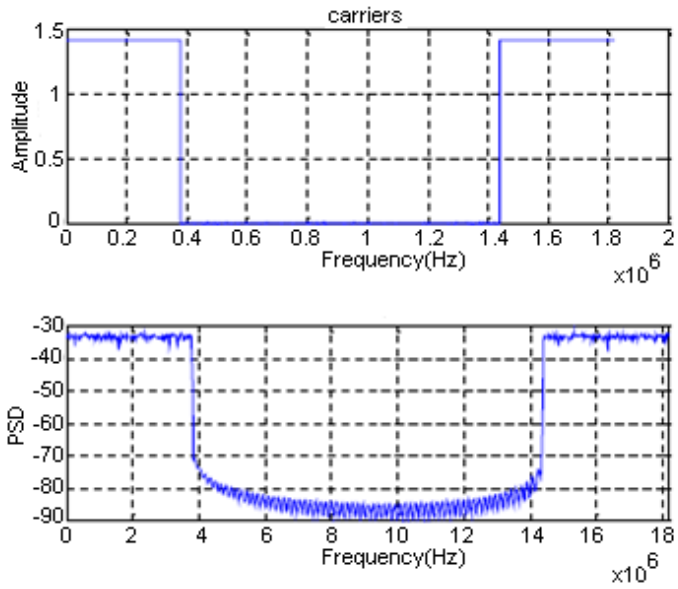

Figure 5.3: Frequency response of the signal carriers

5.2 Complementary Cumulative Distribution Function (CCDF)

In order to see the performance of PAPR reduction, the CCDF curve is plotted for Conventional Selected mapping method. The figures show the effectiveness of the method to reduce the PAPR of the OFDM signal.

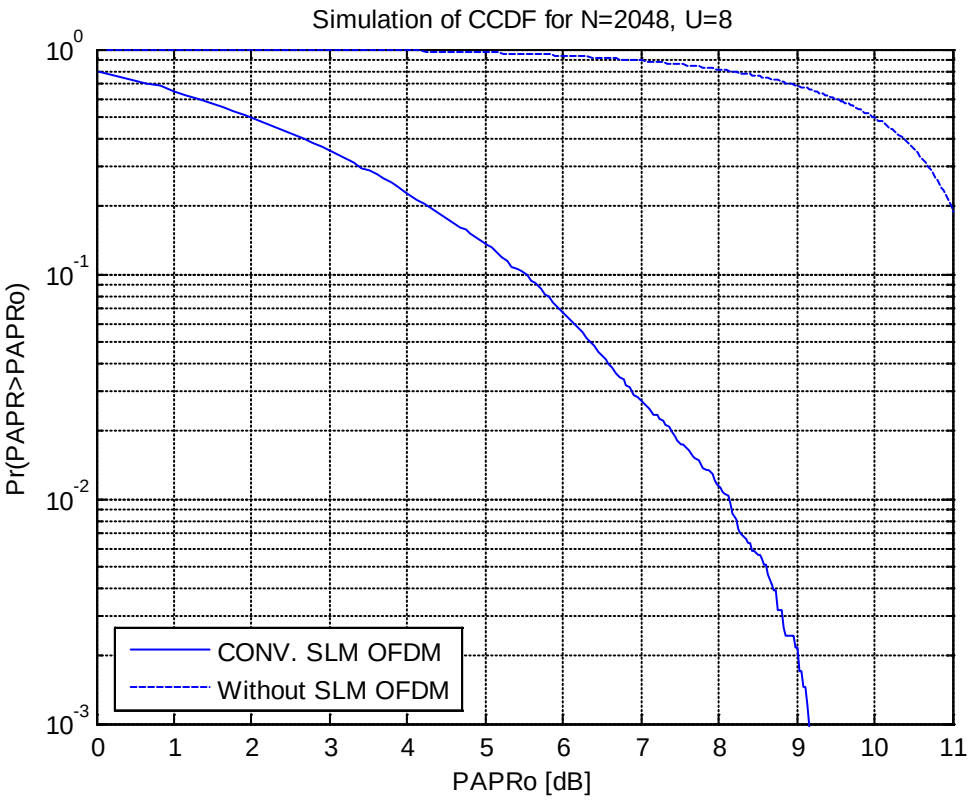

Figure 5.4: CCDF of a randomly generated OFDM signal before and after conventional SLM PAPR reduction method.

We can see from Figure 5.4 that the PAPR of the original OFDM signal is greater than 10dB. If this signal is feed to a non linear device such as high power amplifier, the output will be distorted and resulted in erroneous signal. Transmitting distorted signal leads to loss of the useful information. The conventional Selected Mapping method reduces the PAPR significantly. From the Figure, the probability that the PAPR is greater than 9dB is 0.1%. This probability will be less if the number of phase sequences increase. However, increasing the phase sequence U increases the computational complexity of the system.

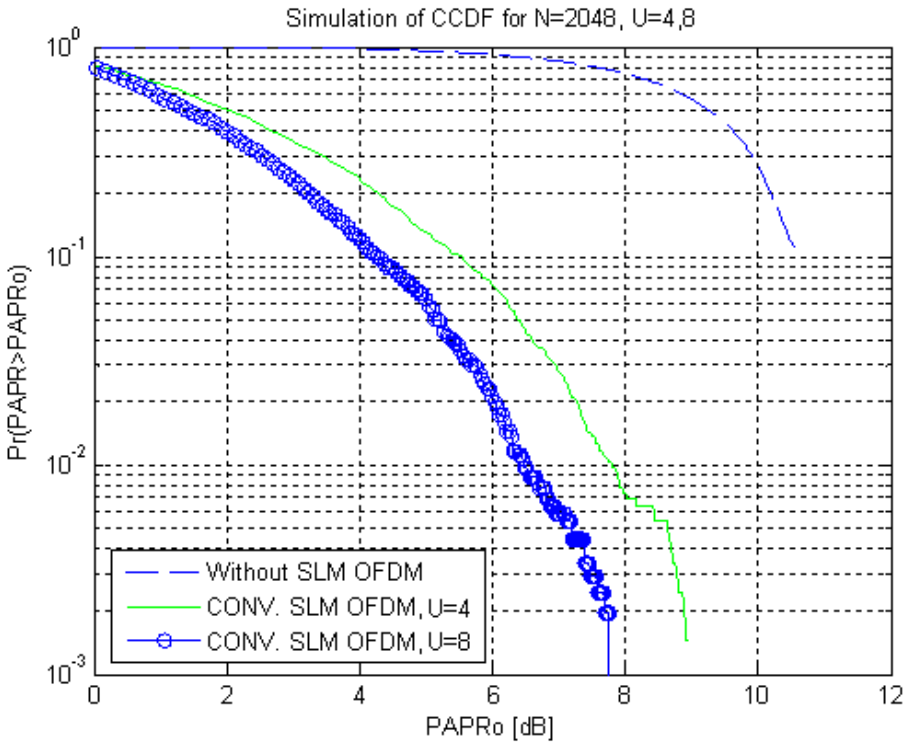

Figure 5.5: CCDF of the SLM PAPR reduction scheme for U= 4, and U= 8.

Figure 5.5 is a plot that demonstrates how improved PAPR can be achieved by increasing the number of mappings (U). Further increase in the number of mapping reduces the PAPR at the expense of computational complexity. It is this computational complexity that restricts the implementation of Selected Mapping.

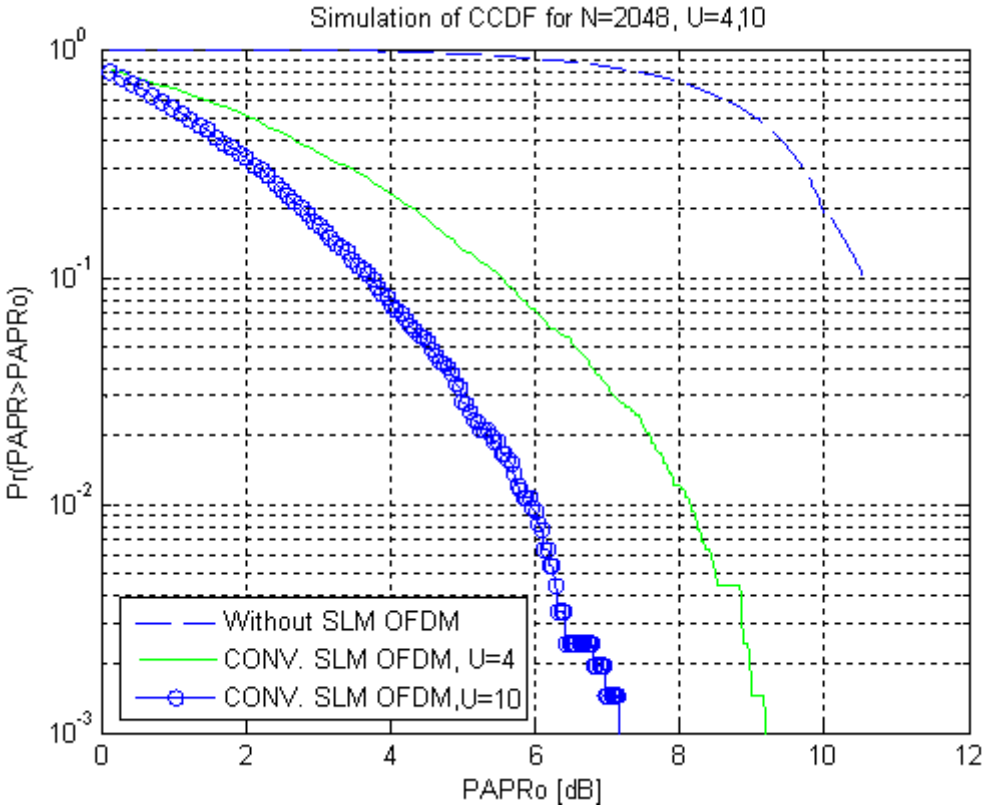

Figure 5.6 : CCDF of the SLM PAPR reduction scheme for U= 4, and U= 10.

5.3 Enhanced Selected Mapping Model

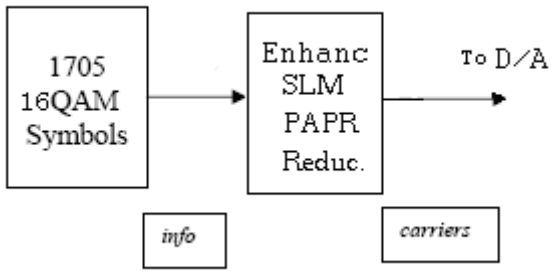

Figure 5.7 : OFDM symbol generation using enhanced SLM.

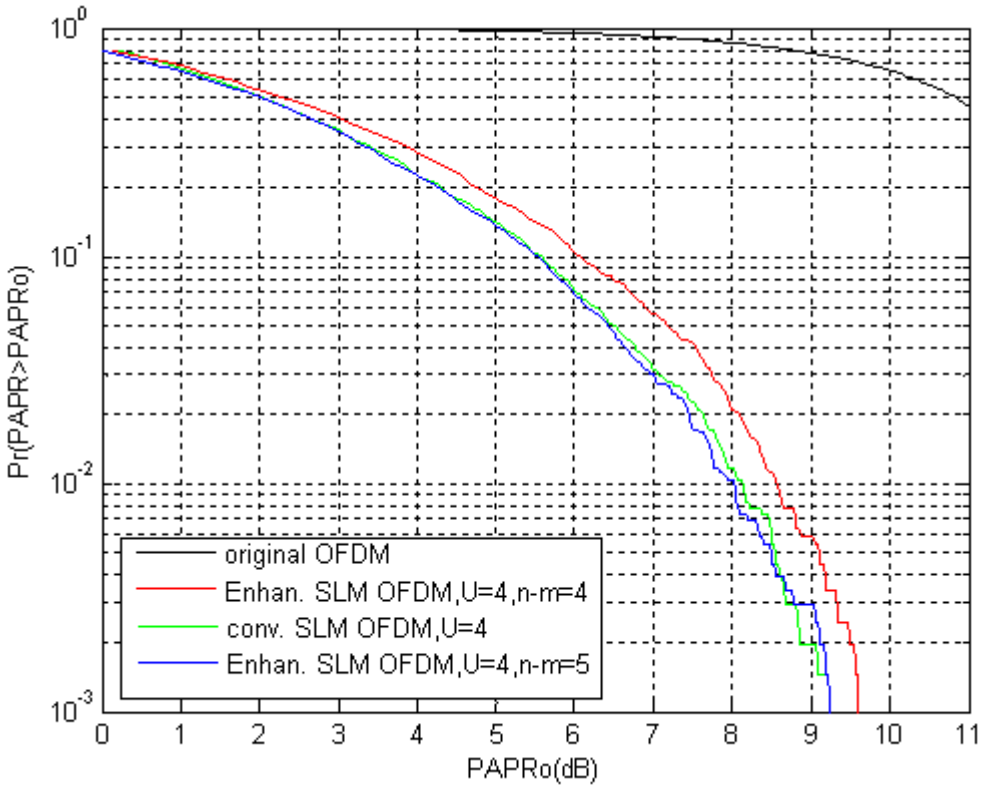

Figure: 5.8 CCDF of the PAPR of enhanced and conventional SLM OFDM scheme for some stages of multiplication with phase sequences when N=2048, U=4, and 16-QAM constellation is used.

The CCDF plot shows that almost both the conventional and enhanced schemes have the same performance when phase sequences are multiplied with only n-m=5 stages from n=11 stages. In this case for N=2048, n=m=5 and U=4, we get a 41% computational complexity reduction. The computational complexity reduction ratio increases as the number of carriers increases. This makes this enhanced scheme to be most suitable for the high data rate OFDM systems.

The figure also shows that n-m= 5 outperforms n-m=4 by less than 1dB. To see how many stages of the IFFT have to be used in common before phase sequencing, we have to perform the simulation for different n-m values. In our case, the simulation is done by comparing with n-m=5 which is the optimal value for the intermediate stage of IFFT.

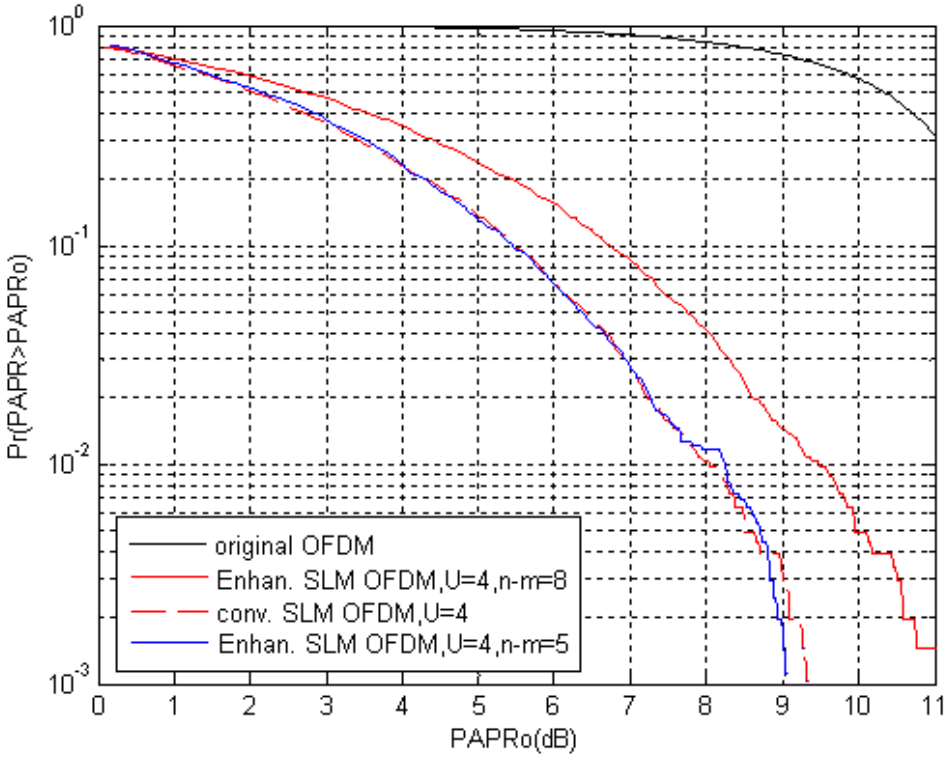

Figure: 5.9 Performance comparison of the enhanced selected mapping scheme when N=2048, $n-m$ =5 and $n-m=8$

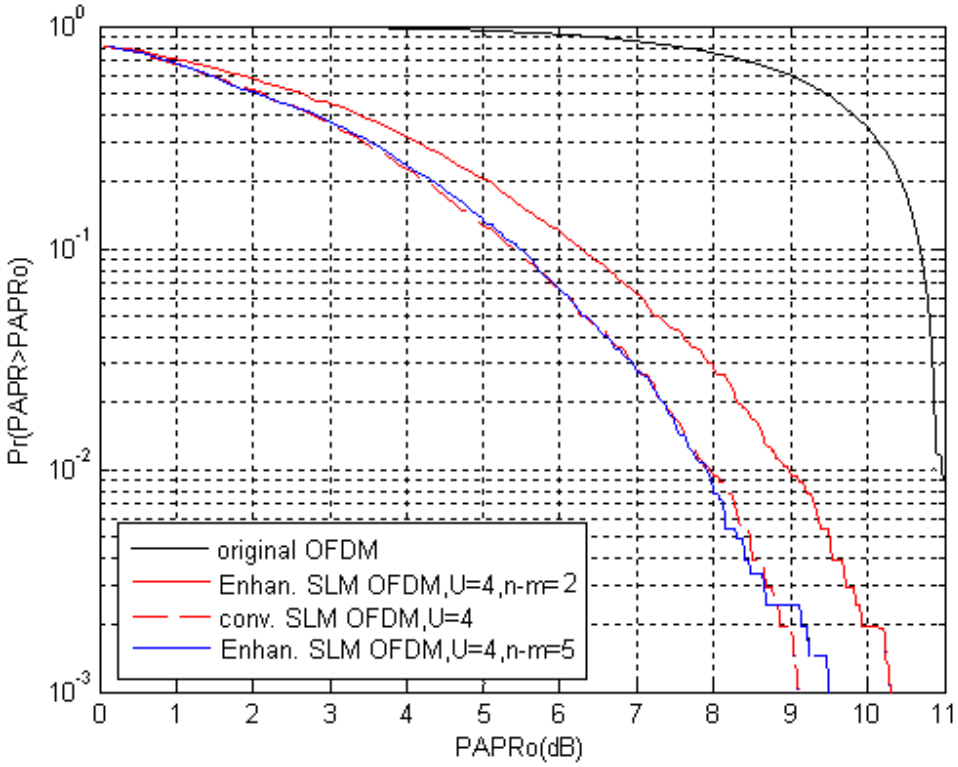

Figure: 5.10 Performance comparison of the enhanced selected mapping scheme when N=2048, $n-m=5$ and $n-m=2$

The above two figures show the simulation results as the stage of multiplication with phase sequences is varied for $n-m=2,\ 5, 8$. From the simulation results, we can say that the optimum value for $n-m$ does not depend on the number of carriers, and the optimal value is around 5. The enhanced scheme with 2048 carriers has almost the same performance compared to the conventional Selected Mapping OFDM scheme.

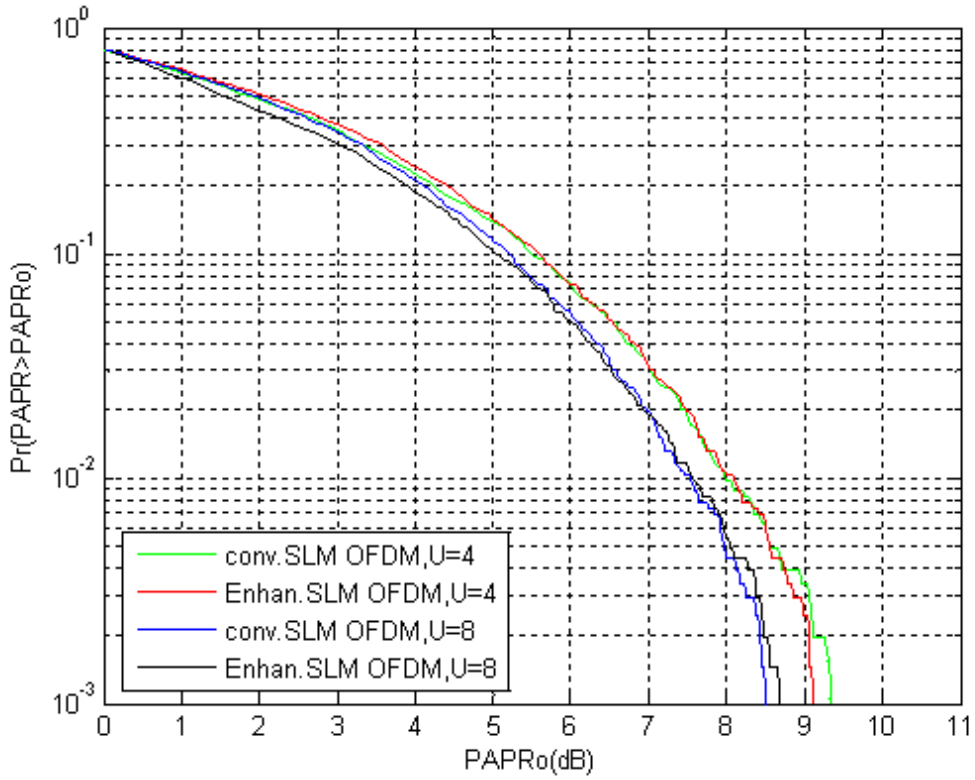

Figure: 5.10 Performance comparison of the enhanced SLM OFDM scheme and the conventional SLM OFDM scheme when N=2048, $n-m=5$ and 16-QAM is used.

As one can see from the above figure, the enhanced Selected Mapping OFDM has almost the same performance of PAPR reduction as that of the conventional Selected Mapping OFDM scheme. In our case when $n-m=5$ and $U=8$, the enhanced SLM OFDM scheme reduces the computational complexity by 48%. If we further increase the number of sequences (*U)* to *16*, nearly 51% computational complexity reduction can be achieved. Thus the practical implementation problem is solved.

CHAPTER VI

CONCLUSION AND FUTURE WORK

6.1 Conclusions

In this thesis an overview of PAPR reduction schemes in OFDM communication has been given. The effectiveness and implementation complexity vary heavily from scheme to scheme. The major PAPR reduction techniques are compared based on their advantages and disadvantages and emphasis is given on Selected Mapping (SLM). The detailed analysis and simulation of this conventional SLM technique is given in this thesis. It is found that computational complexity of conventional SLM OFDM scheme hinders its practical implementation.

The enhanced SLM OFDM with low computational complexity is proposed and its performance is checked for the OFDM DVB-T system of the *IEEE* standard 802.16 [28] intended for mobile reception of digital TV. The simulation results of this technique show that the computational complexity reduces by 48% for 2048 subcarriers and $n\text{-}m=5$. The PAPR reduction performance of the enhanced SLM scheme is almost the same as that of the conventional SLM OFDM scheme. An increased computational complexity reduction is obtained as the number of carriers/subcarriers is increased. Therefore, the enhanced SLM scheme is more suitable for the high data rate OFDM communication systems.

Therefore, the enhanced scheme appears to be the best technique for PAPR reduction. The PAPR reduction is at the expense of a limited reduction of some useful transmission bandwidth. The scheme is also used for metropolitan local area networks (MLAN) OFDM systems. It can be easily adapted to the required performance with a low impact on the overall characteristics of the system.

6.2 Future work

Although this thesis had provided a significant contribution on the PAPR reduction of OFDM communication systems, some aspects of the enhanced SLM technique require a further study. This technique requires side information transmission which needs valuable bandwidth that could be used for sending useful information. So our future study focuses on investigating the effect of errors on reception of side information. Alternatively, we will find mechanisms of avoiding side information transmission. Power savings analysis will also be performed for selected mapping.

Appendix A

More on the OFDM Literature

The first OFDM-like radio to be found in the research literature is the Kineplex system presented by Mosier et.al in 1958 [33]. Developed at the Collins Radio Company, Burbank, CA, the radio used 20 tones separated by 110 Hz, each differentially phase modulated. This paper caused some interest and some controversy as indicated by E. D. Sunde's (Bell Laboratories) comments found at the end of the journal paper. In his 1960 paper [29], H. F. Harmuth, a researcher at General Dynamics, Rochester, NY, suggested multiplexing orthogonal waveforms. Then, in 1967 M. S. Zimmerman et.al described a 34 subcarrier military radio named Kathryn. The first paper to identify the Doppler sensitivity of such a radio was by P. A. Bello [20]. Significant theoretical contributions were made by B. R. Saltzberg and R. W. Chang of Bell Laboratories [24]. In 1970 Chang was issued US patent on OFDM [23]. Weinstein and Ebert, in 1971, where to first to suggest using a DFT for OFDM modulation [37]. This observation was made six years after Cooley and Tukey published details of the fast Fourier transform; these developments were significant since all modern OFDM systems are based on the FFT. A decade passed with little mention of OFDM in the literature.

Then, in the early 80's researchers from IBM's Watson Research Center suggests OFDM for a wireline DSL type application [34]. They were the first to suggest bit loading. Around this time, Japanese researcher suggest OFDM for wireless communications [30]. L. J. Cimini's 1985 paper [22] generated interest when he suggested applying OFDM to mobile systems. In the late 80's and early 90's OFDM received wide interest for the applications of DSL and for wireless digital broadcasting. Kalet and Zervos compared OFDM to single carrier with decision feedback equalization [32]. The acceptance of OFDM into xDSL standards was lead primarily by Stanford University's J. M. Cioffi et al. [25]. Now, OFDM is widely deployed for this consumer electronics application. In terms of digital broadcasting, OFDM has been accepted for the European DAB and DVB standards [27]. OFDM is being applied to indoor wireless local area networks under the IEEE 802.11 and the ETSI HYPERLAN/2 standards [36]. And as mentioned in Chapter 2, OFDM

is being developed for ultra-wideband systems; cellular systems; wireless metropolitan area networks; and for power line communication [26]. Active OFDM research continues. The major focus in the OFDM literature includes OFDM's sensitivity to Doppler, phase noise, carrier frequency offsets, and nonlinearities.

Channel estimation and synchronization techniques are of interest, along with techniques to address the PAPR problem.

APPENDIX B

PRACTICAL OFDM EXAMPLE

DVB-T Example

A detailed description of OFDM can be found in [2] where we can find the expression for one OFDM symbol starting at $t=t_s$ as follows:

$$s(t) = \left\{ \sum_{i=-\frac{N_s}{2}}^{\frac{N_s}{2}} d_{i+N_s/2} \exp(f_c - \frac{i+0.5}{T})(t-t_s) \right\}, \quad t_s \le t \le t_s + T$$
$$s(t) = 0 \quad , t < t_s \ \wedge \ \ t > t_s + T \tag{58}$$

Where d_i are complex modulation symbols, Ns is the number of subcarriers, T the symbol duration, and f the carrier frequency. A particular version of (58) is given in the DVB-T standard as the emitted signal. The expression is

$$s(t) = \mathrm{Re}\left\{ e^{j2\pi f_c t} \sum_{m=0}^{\infty} \sum_{l=0}^{67} \sum_{k=K_{\min}}^{K_{\max}} C_{m,I,k} \cdot \varphi_{m,I,k}(t) \right\} \tag{59}$$

Where

$$\varphi_{m,I,k} = \begin{cases} e^{j2\pi \frac{k'}{T_u}(t-\Delta-l.T_s-68.m.T_s)} & ,(l+68.m).T_s \le t \le (l+68.m+1).T_s \\ 0 & , \quad else \end{cases} \tag{60}$$

k denotes the carrier number;

l denotes the OFDM symbol number;

m denotes the transmission frame number;

K is the number of transmitted carriers;

T_S is the symbol duration;

T_U is the inverse of the carrier spacing;

Δ is the duration of the guard interval;

F_c is the central frequency of the radio frequency (RF) signal;

$k`$ is the carrier index relative to the center frequency,

k` = k-(Kmax + Kmin)/2;

$C_{m,\,o,\,k}$ complex symbol for carrier k of the data symbol no.1 in frame number m;

$C_{m,\,1,k}$ complex symbol for carrier k of the data symbol no.2 in frame number m;

$C_{m,\,67,k}$ complex symbol for carrier k of the data symbol no.68 in frame number m;

This mode of the DVB-T standard is used for mobile reception of digital TV. The transmitted OFDM signal is organized in frames, each having duration T_F. Each frame consists of 68 OFDM symbols. Each symbol is constituted by a set of K=1705 carriers and transmitted with a duration of Ts, composed of a useful part with a duration T_U and a guard interval with a duration Δ.

The numerical values for the OFDM parameters

Parameter	**Value**			
Elementary period T	7/64μs			
Number of carriers	1,705			
Value of carrier number K_{min}	0			
Value of carrier number K_{max}	1704			
Duration T_u	224μs			
Carrier spacing 1/ T_u	4,464 Hz			
Spacing between carriers K_{min} and $k_{max}(K-1)/ T_u$	7.61 MHz			
Allowed Guard interval Δ/T_u	1/4	1/8	1/16	1/32
Duration of symbol part T_u	2,048×T=224 μs			
Duration of Guard interval Δ	512×T 56 μs	256×T 28 μs	128×T 14 μs	64×T 7 μs
Symbol Duration $T_s=\Delta + T_u$	2,560×T 280 μs	2,304×T 252 μs	2,176×T 238 μs	2,112×T 231 μs

IFFT Implementation

The IFFT is usually performed after the data array is phase shifted for peak power reduction. Phase shifting technique is use of selected mapping scheme before D/A and power amplifier. The OFDM spectrum is centered on f_c. This means that sub-carrier 1 is located (7.61/2) MHz to the left of the carrier and sub-carrier 1705 is located (7.61/2) MHz to the right of the carrier. A simple way to achieve centering is to use a 2N-IFFT [1] and T/2 as the elementary period. As you can see from the table, the

OFDM symbol duration T_U is specified considering a 2048-IFFT (N=2048); thus we will use a 4096-IFFT. Next, a suitable simulation period must be selected. T is defined as the elementary period for an OFDM signal. The result is a carrier frequency of around 90 MHz, which is in the range of a VHF channel five, a common TV channel in any city.

Symbols

Set Theory

$\in$	is an element of
$\in$	is not an element of
[·]	closed interval
[·)	open interval
$\{x_n\}_{n=1}^{N}$	set of elements x1, x2, . . . , x_N

Operators and Miscellaneous Symbols

arg(·)	argument
cos(·)	cosine
DFT{·}	discrete Fourier transform
e	2.71828182845905. . .
e(·)	exponential function
exp(·)	exponential function
E{·}	expected value
F{·}(f)	Fourier transform
I_0(·)	0^{th}-order modified Bessel function of the first kind
IDFT{·}	inverse discrete Fourier transform
{·}	imaginary part
j	$\sqrt{-1}$
Max	maximum
min	minimum
ln(·)	natural log
logx(·)	log base x
P(·)	probability
Q(·)	Gaussian Q-function
sinc(·)	sinc function
var{·}	variance
x(t)	x as a function of t
x[i]	discrete-time samples of x at the i^{th} index

$\delta(\cdot)$	delta function
e	3.14159265358. . .
∞	infinity
$\int_a^b(.)dx$	definite integral
$\int(.)dx$	indefinite integral
$\prod_{n=1}^{N}$	multiple product
$\sum_{n=1}^{N}$	multiple sum
$\lvert\cdot\rvert$	absolute value
$(\cdot)^*$	complex conjugate
$\lceil\ \rceil$	ceiling function
$\lfloor\ \rfloor$	floor function
=	equal
$\neq$	not equal
$\leq$	less than or equal to
$\geq$	greater than

REFERENCES

1. N. V. Richard and P. Ramjee, " OFDM for Wireless Multimedia Communications ," Artech House, Boston, 2000.
2. Andrea Goldsmith, "Wireless Communications," Cambridge University Press, Stanford University, 2005.
3. ___, "Orthogonal Frequency Division Multiplexing-Applications for wireless communication," 2001.
4. A. C. Brooks and S. J. Hoelzer, "Design and simulation of Orthogonal Frequency Division Multiplexing (OFDM) Signaling," 2001
5. H. Seung and H. Lee, "Modified Selected Mapping Technique for PAPR reduction of Coded OFDM signal," *IEEE Trans. Broadcasting*, vol. 50, No. 3, Sep. 2004.
6. C. Wang and Y. Ouyang, "Low-Complexity Selected Mapping Schemes for Peak-to-Average Power Ratio Reduction in OFDM Systems," *IEEE Trans. Signal processing*, vol. 53, No. 12, Dec. 2005.
7. Dr. Laszlo Babai, "Hadamard Matrices," Lecture Note, June 2002
8. Ochiai, H. and Imai, H., "Performance analysis of deliberately clipped OFDM signals," *IEEE Trans. Communications*, vol. 50, Jan. 2002.
9. Kim, D. and Stuber, G. L., "Clipping noise mitigation for OFDM by decision-aided reconstruction," *IEEE Communications Letters*, vol. 3, 1999.
10. X. Wang and T. T. Tjhung, "Reduction of Peak-to-Average Power Ratio of OFDM System Using A Companding Technique," *IEEE Transactions On Broadcasting.* Vol.. 45. NO. 3. September 1999.
11. J. Tellado, "Peak to Average Power Reduction for Multicarrier Modulation," Ph.D. dissertation, Stanford Univ., September 1999.
12. D. Farnese, "Techniques for Peak power reduction in OFDM Systems," Msc. Thesis, Chalmers University, 1998.
13. H. F. Harmuth, "On the Transmission of Information by Orthogonal Time Functions," AIEE. Trans., vol. 79, July 1960.
14. Zou, W. Y. and Wu, Y., 'COFDM' : An overview," *IEEE Trans. Broadcasting*, vol. 41, March 1995.

15. H. Dai and H. V. Poor, “Advanced Signal Processing for Power Line Communications,” IEEE Commun. Mag., vol. 41, no. 5, May 2003.
16. Proakis, J. G., *Digital Communications*. New York, NY: McGraw-Hill, 2001.
17. Dinur, N. and Wulich, D., “Peak-toaverage power ratio in high-order OFDM," *IEEE Trans. Communications*, vol. 49, June 2001.
18. van Nee, R. and de Wild, A., “Reducing the peak-to-average power ratio of OFDM," *Proc. IEEE Vehicular Technology Conference*, vol. 3, 1998.
19. S, H. Muller., R. W. Bauml, and et al, *OFDM with reduced Peak-to-Average Power ratio by multiple signal représentation*, IEEE Trans. Commun., vol. 52, no. 2, July 1997.
20. —, “Selective Fading Limitations of the Kathryn Modem and Some System Design Considerations,” IEEE Trans. Commun., Sept. 1965.
21. R. W. Bauml, F. H. Fischer, J. B. Huber, “Reducing the PAPR of Multicarrier Modulation by Selected Mapping,” Erlangen University, Germany.
22. L. J. Cimini, Jr., “Analysis and Simulation of a Digital Mobile Channel Using Orthogonal Frequency Division Multiplexing,” IEEE Trans. Commun., vol. 33, no. 7, July 1985.
23. R. W. Chang, “Orthogonal frequency division multiplexing,” Nov. 14, 1966.
24. —, “Synthesis of band-limited orthogonal signals for multichannel data transmission,” Bell Syst. Tech. J., vol. 45, Dec. 1966.
25. P. S. Chow, J. C. Tu, and J. M. Cioffi, “Performance Evaluation of a Multichannel Transceiver system for ADSL and VHDSL Services,” IEEE J. Select. Areas Commun., vol. 9, Aug. 1991.
26. H. Dai and H. V. Poor, “Advanced Signal Processing for Power Line Communications,” IEEE Commun. Mag., vol. 41, no. 5, May 2003.
27. B. L. Floch, R. Halbert-Lassalie, and D. Castelain, “Digital Sound Broadcasting to Mobile Receivers,” IEEE Trans. Consumer Electron., vol. 35, no. 3, Aug. 1989.
28. OFDM Simulation using MATLAB. Retrieved May 9, 2003, from http://users.ece.gatech.edu/~mai/tutorial/OFDM/Tutorial_web.pdf
29. H. F. Harmuth, “On the Transmission of Information by Orthogonal Time Functions,” AIEE. Trans., vol. 79, July 1960.

30. B. Hirosaki, “An Analysis of Automatic Equalizers for Orthogonally Multiplexed QAM Systems,” IEEE Trans. Commun., vol. com-28, no. 1, Jan. 1980.
31. Ibiquity—Digital Radio. [Online]. Available: http://www.ibiquity.com/
32. I. Kalet, “The Multitone Channel,” IEEE Trans. Commun., vol. 37, no. 2, Feb. 1989.
33. R. R. Mosier and R. G. Clabaugh, “Kineplex, a Bandwidth-Efficient Binary Transmission System,” AIEE Trans., vol. 76, Jan. 1958.
34. A. Peled and A. Ruiz, “Frequency Domain Data Transmission Using Reduced Computational Complexity Algorithms,” in Proc. IEEE Commun., vol. 5, Apr. 1980.
35. A. Loghman, “Analysis of Nonlinear Distortion in Power Amplifiers Using OFDM Signals,” Msc. Thesis, Stockholm,2006.
36. R. van Nee, G. Awater, M. Morikura, H. Takanashi, M. Webster, and K. W. Halford, “New High-Rate Wireless LAN Standards,” IEEE Commun. Mag., Dec. 1999.
37. S. B. Weinstein and P. M. Ebert, “Data Transmission by Frequency-Division Multiplexing Using the Discrete Fourier Transform,” IEEE Trans. Commun. Technol., vol. 19, no. 5, Oct. 1971.
38. Lei X., Li S., and Tang Y., “OFDM clipping noise mitigation by a novel minimum clipping power loss scheme," *IEEE Proc. Vehicular Technology Conference*, vol. 4, Oct. 2003.
39. Baxley, R. J. and Zhou, G. T., “Assessing peak-to-average power ratios for communications applications," *Proc. IEEE MILCOM Conference*, Oct. 2004.
40. Rappaport, T., *Wireless Communications*. Prentice Hall, 2002.

Declaration

I, the undersigned, declare that this thesis is my original work, has not been presented for a degree in this or any other university, and all sources of materials used for the thesis have been acknowledged.

Name: Mengistu Abera

Signature: _____

Place: Addis Ababa

Date of submission: _____

This thesis has been submitted for examination with my approval as a university advisor.

Dr.-Ing. Hailu Ayele _____

Advisor's Name Signature